2010-05

Adaptive Vision-Based Guidance Law with Guaranteed Performance Bounds

Ma, L.; Cao, C.; Hovakimyan, N.; Dobrokhodov, V.; Kaminer, I.I

AIAA

Ma, Lili, et al. "Adaptive vision-based guidance law with guaranteed performance bounds." Journal of guidance, control, and dynamics 33.3 (2010): 834-852.
http://hdl.handle.net/10945/62673

JOURNAL OF GUIDANCE, CONTROL, AND DYNAMICS
Vol. 33, No. 3, May–June 2010

Adaptive Vision-Based Guidance Law with Guaranteed Performance Bounds

Lili Ma*
Wentworth Institute of Technology, Boston, Massachusetts 02135
Chengyu Cao†
University of Connecticut, Storrs, Connecticut 06269
Naira Hovakimyan‡
University of Illinois at Urbana–Champaign, Urbana, Illinois 61801
and
Vladimir Dobrokhodov§ and Isaac Kaminer§
Naval Postgraduate School, Monterey, California 93943

DOI: 10.2514/1.46287

This work discusses vision-based tracking of a ground vehicle moving with unknown time-varying velocity. The follower unmanned aerial vehicle is equipped with a single camera. The control objective is to regulate the two-dimensional horizontal range between the unmanned aerial vehicle and the target to a constant. The contribution of this paper has two distinct features. The developed guidance law uses the estimates of the target's velocity obtained from a fast-estimation scheme. It is shown that the fast-estimation scheme has guaranteed performance bounds and the tracking performance bound can be explicitly derived as a function of the estimation error. The performance bounds imply that the signals of the closed-loop adaptive system remain close to the corresponding signals of a bounded closed-loop reference system, both in transient and steady-state responses. The reference system is introduced solely for the purpose of analysis. This paper also analyzes the stability and the performance degradation of the closed-loop adaptive system in the presence of out-of-frame events, when continuous extraction of the target's information is not feasible due to failures in the image-processing module. The feedback loop is then closed using the frozen estimates. The out-of-frame events are modeled as brief instabilities. A sufficient condition for the switching signal is derived that guarantees graceful degradation of performance during target loss. The results build upon the earlier-developed fast-estimation scheme of the target's velocity, the inverse-kinematics-based guidance law, and insights from switching systems theory.

I. Introduction

REFERENCES [1–8] have reported theoretical and experimental results on a vision-based tracking and motion estimation system for a small unmanned aerial vehicle (UAV) tasked to follow a ground target using a single camera. In the system, the UAV flies autonomously along a predefined search pattern, while a gimbal operator on the ground may select a target of interest using a joystick that steers the onboard gimballed camera. Real-time video along with the UAV-gimbal telemetry are transmitted to the ground station wirelessly. Once the target is selected, the UAV and the camera automatically track the target. The system also performs real-time estimation of the target's unknown velocity using UAV-gimbal telemetry data and the extracted target position on the image plane. For more information on the flight system, please refer to [2,3,7] and the references therein.

Figure 1 shows the graphical illustration of the vision-based target-tracking scenario, where $\{B\}$, $\{C\}$, and $\{I\}$ represent the body-fixed, camera, and inertial coordinate systems. Let $\rho(t)$ denote the 2-D horizontal range between the UAV and the target. The control objective is to regulate $\rho(t)$ to ρ_d, where ρ_d is a given desired 2-D horizontal range between the UAV and the target. For simplicity, ρ_d is assumed to be constant. For this system, the available measurements are listed below:

1) Visual measurements $u(t)$ and $v(t)$ of the target's center are extracted by an image-processing algorithm.

2) Relative altitude $h(t)$ between the UAV and the target is obtained by georeferencing the image captured by the onboard camera with a given database.

3) UAV information is obtained from onboard sensors, such as the UAV's velocity and orientation.

Although many of the existing large UAV systems are capable of performing complex missions involving target geolocation and tracking, their cost is prohibitively high and, as a result, their operational availability is limited. Moreover, traditional operational concept in the task of vision-only target tracking and UAV navigation necessarily involves at least two operators to perform the target tracking and to establish coordinated UAV motion around the target. This task becomes practically impossible to accomplish in the presence of the intermittent target loss, due to a variety of conditions, including rapid change of lighting and communication interference. The initial development in [1] was specifically pointed to the difficulty of the operators' coordination in performing those tasks and provided an initial framework that essentially eliminated the need for a UAV pilot to leave the operator of the camera to fly the entire system. The developed system in [1] was limited by the assumption of a target moving with unknown constant velocity. In this paper, the target's velocity is relaxed to be time-varying. Estimates of the target's time-varying velocity is obtained through a fast-estimation scheme. An inverse-kinematic-based controller is designed to regulate $\rho(t)$ to ρ_d, using the velocity estimates. How the

Presented as Paper 7445 at the AIAA Guidance, Navigation, and Control Conference and Exhibit, Honolulu, HI, 18–21 August 2008; received 9 July 2009; revision received 13 January 2010; accepted for publication 17 January 2010.

*Assistant Professor, Department of Electronics and Mechanical. Member AIAA (Corresponding Author).
†Assistant Professor, Department of Mechanical Engineering. Member AIAA.
‡Professor, Mechanical Science and Engineering. Member AIAA.
§Member AIAA.

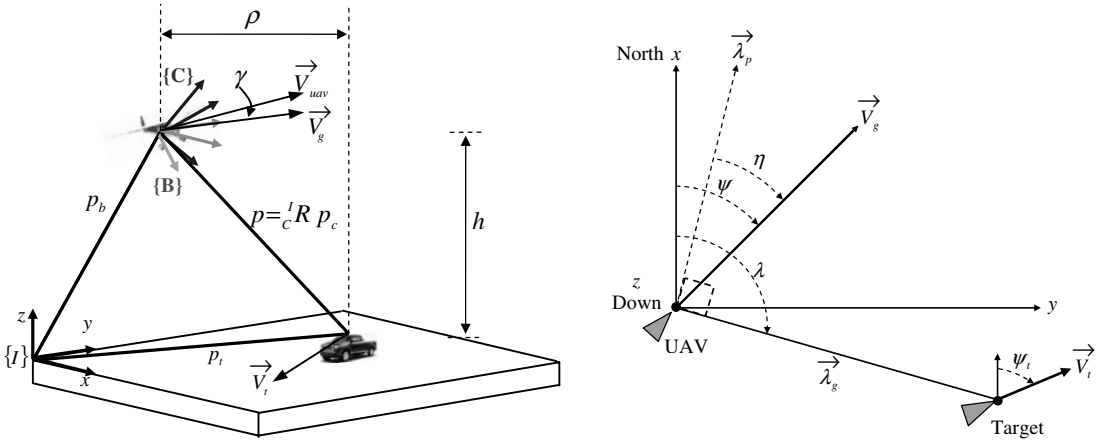

a) 3D demonstration **b) 2D demonstration**

Fig. 1 Relative kinematics of UAV-target motion.

estimation performance bound affects the tracking performance is also analyzed.

In vision-based applications, continuous extraction of the target's information is often unavailable, due to environmental factors, limited field of view of the camera, or failure in the image-processing module. These phenomena are commonly referred to as out-of-frame events [5]. The out-of-frame event cannot be avoided, due to the complexity of a real application scenario. Stability and performance degradation of the system in the presence of target loss, or out-of-frame events, is addressed in this paper. The idea is to use the latest available estimate for the unknown parameters during the target loss. The effects of the out-of-frame events on the estimation and, further, on the target tracking are analyzed and presented. A sufficient condition on the duration of the out-of-frame event is derived that guarantees stability and desired performance. The closed-loop system is viewed as a switching system that switches between one subsystem with *continuous* visual measurements and the other subsystem with *frozen* estimates. The analysis is motivated by [5] and is cast into the framework of switching systems theory [9].

The contribution of the paper is twofold. First, it presents a guidance law that uses the estimate of the target's time-varying velocity, obtained from a fast-estimation scheme. Next, it analyzes the performance of the closed-loop system in the presence of out-of-frame events. A sufficient condition for stability is derived, which relates the dwell time to the design parameters of the feedback law and can be used for improvement of the image-processing algorithm.

The paper is organized as follows. Section II describes the vision-based ground target-tracking problem. Essentials of motion estimation of the target's unknown time-varying velocity are reviewed in Sec. III. Section IV presents the inverse-kinematics-based guidance law and shows that the resulting closed-loop adaptive system bears a close resemblance to a reference system, upon proper selection of the controller gains, both in transient and steady-state responses. In Sec. V, the out-of-frame events are addressed. A sufficient condition on the out-of-frame switching signal is identified to ensure stability and tracking performance. Simulation results are given in Sec. VI. Finally, Sec. VII concludes the paper.

II. Problem Formulation

Let $p(t) = [p_x(t), p_y(t), p_z(t)]^\top$ be the position of the target with respect to the UAV in the inertial frame, let p_c be the relative position of the target and the UAV in the camera's coordinate frame, and let $h(t)$ denote the relative altitude of the UAV above the target. Let $V_{\text{uav}}(t)$ be the UAV's velocity and let $V_g(t)$ be the projection of $V_{\text{UAV}}(t)$ onto the horizontal plane. Denoting the UAV flight-path angle by $\gamma(t)$, one has $V_g(t) = V_{\text{UAV}}(t)\cos\gamma(t)$. Let $V_t(t)$ and $\psi_t(t)$ be the amplitude and the orientation of the target's velocity $\omega(t) = [\omega_1(t), \omega_2(t)]^\top$ in the horizontal plane, and let $V_h(t)$ be the rate of change of target elevation. Let $\eta(t)$ denote the angle between the UAV's velocity vector and the vector perpendicular to the line-of-sight vector, as shown in Fig. 1. The kinematic equations for a UAV tracking a target can be written as [2–5,7]:

$$\begin{aligned}\dot{\rho}(t) &= -V_g(t)\sin\eta(t) + V_t(t)\sin[\psi_t(t) - (\psi(t) - \eta(t))] \\ &= \beta_1(\omega(t))\sin(\eta(t) + \beta_2(\omega(t))), \quad \rho(0) = \rho_0\end{aligned} \tag{1a}$$

$$\begin{aligned}\dot{\eta}(t) = &-\frac{V_g(t)\cos\eta(t) - V_t(t)\cos[\psi_t(t) - (\psi(t) - \eta(t))]}{\rho(t)} \\ &+ \dot{\psi}(t), \quad \eta(0) = \eta_0\end{aligned} \tag{1b}$$

$$\dot{p}(t) = -\begin{bmatrix} V_g(t)\sin\psi(t) \\ V_g(t)\cos\psi(t) \\ V_{\text{UAV}}(t)\sin\gamma(t) \end{bmatrix} + \begin{bmatrix} V_t(t)\sin\psi_t(t) \\ V_t(t)\cos\psi_t(t) \\ V_h(t) \end{bmatrix} \tag{1c}$$

where

$$\begin{cases} \beta_1(\omega(t)) = \text{sign}(\rho_s(t))\sqrt{\rho_s^2(t) + \rho_c^2(t)} \\ \beta_2(\omega(t)) = \tan^{-1}\left(\frac{\rho_c(t)}{\rho_s(t)}\right) \\ \rho_s(t) = -V_g(t) + V_t(t)\cos(\psi_t(t) - \psi(t)) \\ \rho_c(t) = V_t(t)\sin(\psi_t(t) - \psi(t)) \\ V_t(t) = \sqrt{\omega_1^2(t) + \omega_2^2(t)} \\ \psi_t(t) = \tan^{-1}\left(\frac{\omega_1(t)}{\omega_2(t)}\right) \end{cases} \tag{2}$$

The assumptions can be summarized as follows:

1) $V_g(t) > V_t(t)$.

2) $V_g(t)$ and $\psi(t)$ denote the UAV's velocity and yaw angle that are available from the onboard sensors.

3) $\dot{\psi}(t)$ denotes the UAV's yaw rate and is the control input to be designed.

4) $V_t(t)$ and $\psi_t(t)$ denote the target's time-varying velocity and heading angle, which are unknown and time-varying and will be estimated. These two quantities cannot be continuously measured during the out-of-frame events.

5) Note that $\rho(t)$ and $\eta(t)$ can be computed from the visual measurements $u(t)$ and $v(t)$ via algebraic relationships. Recall that $u(t)$ and $v(t)$ denote the coordinates of the target's center, extracted by the image-processing module. Specifically, $\rho(t)$ can be computed as $\rho(t) = h(t)\sqrt{u^2(t) + v^2(t)}$, where the camera's focal length has

been assumed to be 1 without loss of generality. From Fig. 1b, it can be noted that the signal $\eta(t)$ is also related to the visual measurements. Thus, the signals $\rho(t)$ and $\eta(t)$ cannot be continuously measured during the out-of-frame events.

6) The relative position $p(t)$ can be calculated as

$$p(t) = \begin{bmatrix} p_x(t) \\ p_y(t) \\ p_z(t) \end{bmatrix} = {}^{I}_{C}R\, p_c(t) = \left(\frac{h(t)}{-u(t)\sin\theta(t) + v\sin\varphi(t)\cos\theta(t) + \cos\varphi(t)\cos\theta(t)} \right) {}^{I}_{C}R \times \begin{bmatrix} u(t) \\ v(t) \\ 1 \end{bmatrix} \tag{3}$$

where ${}^{I}_{C}R$ denotes the coordinate transformation from the camera frame to the inertial frame, and $\varphi(t)$ and $\theta(t)$ represent the UAV's (known) roll and pitch Euler angles for the rotation matrix ${}^{I}_{C}R$.

The control objective is to regulate $\rho(t)$ to ρ_d, where ρ_d is a given desired 2-D horizontal range between the UAV and the target. For simplicity, ρ_d is a constant. Note that the relative altitude $h(t)$ is not regulated in this paper. The UAV altitude can be straightforwardly controlled by the onboard autopilot.

The proposed guidance law uses a terrain database and an off-the-shelf image-processing algorithm for estimation of the target's time-varying velocity. Uncertainties in these measurements will affect the estimation performance. To facilitate the design and the analysis, it is assumed that both the target geolocation and the image feature extraction exhibit bounded errors. Further, the UAV's velocity $V_g(t)$ and yaw angle $\psi(t)$ are assumed to be precisely known.

III. Target Motion Estimation

Vision-based sensors are used for being low-cost, lightweight, and passive, but require a robust estimation scheme. The extended Kalman filter (EKF) has been used widely for this purpose [10–15]. Application of the EKF requires linearization about the desired trajectory and is very sensitive to initial errors [16–18]. Improvements of EKF performance with application to obstacle avoidance have been reported in [16,17,19] by using unscented Kalman filters and sigma-point Kalman filters. However, boundedness of the estimation error cannot be guaranteed from application of the EKF or its variations. Our designed controller uses estimates of the target's velocity. For the purpose of completeness, some essential details of target motion estimation are reviewed in this section.

Let $x(t) = [p_x(t), p_y(t)]^\top$, where $p_x(t)$ and $p_y(t)$ denote the x and y components of the relative position between the UAV and the ground target in the inertial frame. Note that $x(t)$ can be computed from the UAV's onboard sensors and visual measurements of the target, as given in Eq. (3). Equation (1c) leads to

$$\begin{bmatrix} \dot{p}_x(t) \\ \dot{p}_y(t) \end{bmatrix} = -V_g(t) \begin{bmatrix} \sin\psi(t) \\ \cos\psi(t) \end{bmatrix} + V_t(t) \begin{bmatrix} \sin\psi_t(t) \\ \cos\psi_t(t) \end{bmatrix} \tag{4}$$

Let

$$\omega(t) = V_t(t) \begin{bmatrix} \sin\psi_t(t) \\ \cos\psi_t(t) \end{bmatrix}, \qquad \omega(0) = \omega_0 \tag{5}$$

Since the moving ground target is a mechanical system, subject to Newton's second law, its velocity and acceleration are bounded. Therefore, there exist constants μ_ω and d_ω such that

$$\|\omega(t)\| \le \mu_\omega < \infty, \quad \forall\ t \ge 0 \qquad \|\dot{\omega}(t)\| \le d_\omega < \infty, \quad \forall\ t \ge 0 \tag{6}$$

The estimates of target's velocity $V_t(t)$ and heading angle $\psi_t(t)$ (denoted by $\hat{V}_t(t)$ and $\hat{\psi}_t(t)$, respectively) can be obtained through the following steps [7,20,21]:

1) The state predictor is

$$\dot{\hat{x}}(t) = A_m \tilde{x}(t) - V_g(t) \begin{bmatrix} \sin\psi(t) \\ \cos\psi(t) \end{bmatrix} + \hat{\omega}(t)$$
$$\tilde{x}(t) = \hat{x}(t) - x(t), \qquad \hat{x}(0) = x_0 \tag{7}$$

where A_m is a known Hurwitz matrix.

2) The update law is

$$\dot{\hat{\omega}}(t) = \Gamma_c\, \mathrm{Proj}(\hat{\omega}(t), -P\tilde{x}(t)), \qquad \hat{\omega}(0) = \hat{\omega}_0 \tag{8}$$

where $\Gamma_c \in \mathbb{R}^+$ determines the adaptation gain, chosen sufficiently large to ensure fast convergence, and P is the solution of the algebraic equation $A_m^\top P + PA_m = -Q$ for some choice of matrix $Q > 0$.

3) For the low-pass filter, let

$$\omega_r(s) = C(s)\omega(s), \qquad \omega_r(0) = \hat{\omega}_0 \tag{9a}$$

$$\omega_e(s) = C(s)\hat{\omega}(s), \qquad \omega_e(0) = \hat{\omega}_0 \tag{9b}$$

where $C(s)$ is a diagonal matrix, whose ith diagonal element $C_i(s)$ is a strictly proper, stable, transfer function with low-pass gain $C_i(0) = 1$ for $i = 1, 2$, with s being the Laplace variable. Let

$$C_i(s) = \frac{c}{s+c}, \qquad i = 1, 2, \qquad c > 0 \tag{10}$$

4) For extraction of $\hat{V}_t(t)$ and $\hat{\psi}_t(t)$ from $\omega_e(t)$,

$$\hat{V}_t(t) = \sqrt{\omega_{e_1}^2(t) + \omega_{e_2}^2(t)}, \qquad \hat{\psi}_t(t) = \tan^{-1}\left(\frac{\omega_{e_1}(t)}{\omega_{e_2}(t)} \right) \tag{11}$$

The fast estimator ensures that $\omega_e(t)$ estimates the unknown signal $\omega(t)$ with the final precision [20,21]:

$$\lim_{t\to\infty} \|\omega_e - \omega\|_{\mathcal{L}_\infty} \le \|\omega_e - \omega_r\|_{\mathcal{L}_\infty} + \|\omega_r - \omega\|_{\mathcal{L}_\infty} \le \frac{\gamma_c}{\sqrt{\Gamma_c}} + \underbrace{\|1 - C(s)\|_{\mathcal{L}_1} \|\omega\|_{\mathcal{L}_\infty}}_{\gamma_{c\omega}} \tag{12}$$

where $\|\cdot\|_{\mathcal{L}_\infty}$ denotes the $\mathcal{L}_\infty$-norm of a signal, $\|\cdot\|_{\mathcal{L}_1}$ denotes the $\mathcal{L}_1$-norm of the system, and

$$\gamma_c = \|C(s)H^{-1}(s)\|_{\mathcal{L}_1} \sqrt{\frac{\omega_m}{\lambda_{\min}(P)}}$$
$$\omega_m = 4\mu_\omega^2 + 4\mu_\omega d_\omega \frac{\lambda_{\max}(P)}{\lambda_{\min}(Q)}$$
$$H(s) = (s\mathbb{I} - A_m)^{-1} \tag{13}$$

where $\mathbb{I}$ denotes an identity matrix of appropriate dimension. Definitions of $\|\cdot\|_{\mathcal{L}_\infty}$ and $\|\cdot\|_{\mathcal{L}_1}$ are reviewed in Appendix A.

When the transients of $C(s)$ due to the initial condition $(\hat{\omega}(0) - \omega(0))$ die out, $\omega_e(t)$ estimates $\omega(t)$ with the final precision given in inequality (12). It was shown in [22] (Proposition 11, pages 103–104) that if the Hurwitz matrix A_m in Eq. (7) is a diagonal matrix of the form $A_m = \mathrm{diag}(a_{m_1}, a_{m_2})$, where a_{m_1} and a_{m_2} are negative constants, then for the choice of $C(s)$ in Eq. (10),

$$\|C(s)H^{-1}(s)\|_{\mathcal{L}_1} = \left\| \frac{c}{s+c}(s\mathbb{I} - A_m)^{-1} \right\|_{\mathcal{L}_1} = \frac{1}{\min\{|a_{m_1}|, |a_{m_2}|\}} \tag{14}$$

It follows from Eqs. (12–14) that

$$\|\omega_e - \omega_r\|_{\mathcal{L}_\infty} \le \frac{1}{\sqrt{\Gamma_c}\min\{|a_{m_1}|, |a_{m_2}|\}} \sqrt{\frac{\omega_m}{\lambda_{\min}(P)}} \tag{15}$$

which is independent of c in Eq. (10). Thus, selection of the bandwidth of $C(s)$ and the adaptation gain Γ_c is independent of each other. Increasing the adaptation gain Γ_c reduces the term $\|\omega_e -$

$\omega_r\|_{\mathcal{L}_\infty}$ to be arbitrarily small. Note that increasing the adaptation gain Γ_c requires faster computation and a smaller integration step. Further, increasing the bandwidth of $C(s)$ ensures that $\omega_r(t)$ tracks $\omega(t)$ arbitrarily closely, both in transient and steady-state responses. The transient of $\omega(t) - \omega_r(t)$ can be quantified as [21]

$$\|\omega(t) - \omega_r(t)\|_\infty \le \|\omega_0 - \hat{\omega}_0\|_\infty e^{-ct} + \gamma_{c\omega}, \quad \forall\ t \ge 0 \tag{16}$$

IV. Guaranteed Transient and Steady-State Performance of the Vision-Based Guidance Law

Consider Eqs. (1a) and (1b). The following guidance law was designed in our early work to regulate $\rho(t)$ to ρ_d in the presence of continuous visual measurements [7,8,23]:

$$\begin{cases} \dot{\psi}(t) = \frac{V_g(t)\cos\eta(t) - \hat{V}_t(t)\cos[\hat{\psi}_t(t) - (\psi(t) - \eta(t))]}{\rho(t)} - k_2(\eta(t) - \eta_d(\omega_e(t), \rho(t))), \\ \eta_d(\omega_e(t), \rho(t)) = \sin^{-1}\left(\frac{-k_1(\rho(t) - \rho_d)}{\beta_1(\omega_e(t))}\right) - \beta_2(\omega_e(t)) \end{cases} \tag{17}$$

where $k_i > 0$ (for $i = 1, 2$) are the design gains. The signal $\omega_e(t)$ denotes the estimation of $\omega(t)$, obtained through Eqs. (7–11). The signals $\hat{V}_t(t)$ and $\hat{\psi}_t(t)$ are the estimated amplitude and heading angle of the target's velocity.

A. Closed-Loop Reference System

Consider the following closed-loop reference system, with its control signal and system response being defined as

$$\begin{cases} \dot{\rho}_r(t) = \beta_1(\omega(t))\sin(\eta_r(t) + \beta_2(\omega(t))),\ \rho_r(0) = \rho_0 \\ \dot{\eta}_r(t) = -\frac{V_g(t)\cos\eta_r(t) - V_t(t)\cos[\psi_t(t) - (\psi(t) - \eta_r(t))]}{\rho_r(t)} \\ \qquad + \dot{\psi}_r(t),\ \eta_r(0) = \eta_0 \\ \dot{\psi}_r(t) = \frac{V_g(t)\cos\eta_r(t) - V_r(t)\cos[\psi_r(t) - (\psi(t) - \eta_r(t))]}{\rho_r(t)} \\ \qquad - k_2(\eta_r(t) - \eta_d(\omega_r(t), \rho_r(t))) \\ \eta_d(\omega_r(t), \rho_r(t)) = \sin^{-1}\left(\frac{-k_1(\rho_r(t) - \rho_d)}{\beta_1(\omega_r(t))}\right) - \beta_2(\omega_r(t)) \end{cases} \tag{18}$$

where $\omega_r(t)$ is given in Eq. (9a) and

$$V_r(t) = \sqrt{\omega_{r_1}^2(t) + \omega_{r_2}^2(t)}, \qquad \psi_r(t) = \tan^{-1}\left(\frac{\omega_{r_1}(t)}{\omega_{r_2}(t)}\right) \tag{19}$$

Note that the reference system in Eq. (18) is not implementable, since it uses the unknown signal $\omega_r(t)$. This closed-loop reference system is only used for the purpose of analysis and it does not affect the implementation of the adaptive controller in Eq. (17). The purpose of introducing this reference system is to characterize both the transient and steady-state performance of the closed-loop adaptive system, defined by application of the controller in Eq. (17) to the system in Eq. (1). This is achieved by first characterizing the transient and steady-state performance of the closed-loop reference system in Eq. (18) (to be shown next) and then demonstrating that the signals of the adaptive system can be designed to stay arbitrarily close to the corresponding signals of this reference system, upon proper selection of the controller gains within an appropriate domain of attraction (to be shown in Sec. IV.D).

First consider boundedness of the signals that will be used in establishing the stability of the closed-loop reference system in Eq. (18). Let

$$f(t) = \frac{-k_1(\rho_r(t) - \rho_d)}{\beta_1(\omega_r(t))} \tag{20}$$

and compute $\dot{\eta}_r(\omega_r(t), \rho_r(t))$ from Eq. (18):

$$\begin{aligned} &\dot{\eta}_d(\omega_r(t), \rho_r(t)) \\ &= \frac{1}{\sqrt{1 - \frac{k_1^2(\rho_r(t) - \rho_d)^2}{\beta_1^2(\omega_r(t))}}} \frac{-k_1\dot{\rho}_r(t)\beta_1(\omega_r(t)) + k_1(\rho_r(t) - \rho_d)\dot{\beta}_1(\omega_r(t))}{\beta_1^2(\omega_r(t))} \\ &- \dot{\beta}_2(\omega_r(t)) \\ &= \frac{1}{\sqrt{1 - f^2(t)}}\left(\frac{-k_1\dot{\rho}_r(t)}{\beta_1(\omega_r(t))} + f(t)\frac{\dot{\beta}_1(\omega_r(t))}{\beta_1(\omega_r(t))}\right) - \dot{\beta}_2(\omega_r(t)) \end{aligned} \tag{21}$$

It can be seen from Eqs. (2) and (18) that $\dot{\rho}_r(t)$ is bounded. Bounded $\omega_r(t)$ implies that $\beta_1(\omega_r(t))$, $\beta_2(\omega_r(t))$, $\dot{\beta}_1(\omega_r(t))$, and $\dot{\beta}_2(\omega_r(t))$ are also bounded. It follows from Eq. (21) that if $|f(t)| \le 1 - \epsilon$ for $\epsilon \in (0, 1]$, there exist finite numbers M_{d1}, M_{d2}, and $M_d(k_1)$ such that

$$|\dot{\eta}_d(\omega_r(t), \rho_r(t))| < M_{d1}k_1 + M_{d2} \triangleq M_d(k_1) \tag{22a}$$

In addition, when $\rho_r(t) \ge \gamma_b$, where γ_b is a positive constant, there exists finite constant M_{ρ_r}, such that

$$\left|\frac{V_t(t)\cos[\psi_t(t) - (\psi(t) - \eta_r(t))] - V_r(t)\cos[\psi_r(t) - (\psi(t) - \eta_r(t))]}{\rho_r(t)}\right| < M_{\rho_r} \tag{22b}$$

Further, note that $\omega(t)$, $\omega_r(t)$, $V_t(t)$, $\psi_t(t)$, $V_r(t)$ and $\psi_r(t)$ are bounded signals. It can be shown that the functions $\beta_1(t)$ and $\beta_2(t)$ are Lipschitz-continuous. Therefore, there exist finite constants μ_{β_1}, μ_{β_2}, M_t, M_{β_1}, $M_{\beta_{1r}}$, and $L_{\beta_{1r}}$, such that $\forall\ t \ge 0$,

$$\begin{aligned} &|V_t(t)| < M_t, \quad |\beta_1(\omega(t))| < M_{\beta_1}, \quad L_{\beta_{1r}} < |\beta_1(\omega_r(t))| < M_{\beta_{1r}} \\ &|\beta_1(\omega(t)) - \beta_1(\omega_r(t))| < \mu_{\beta_1}\|\omega(t) - \omega_r(t)\|_\infty \\ &\quad < \mu_{\beta_1}(\|\omega_0 - \hat{\omega}_0\|_\infty e^{-ct} + \gamma_{c\omega}) \\ &|\beta_2(\omega(t)) - \beta_2(\omega_r(t))| < \mu_{\beta_2}\|\omega(t) - \omega_r(t)\|_\infty \\ &\quad < \mu_{\beta_2}(\|\omega_0 - \hat{\omega}_0\|_\infty e^{-ct} + \gamma_{c\omega}) \end{aligned} \tag{22c}$$

where $\gamma_{c\omega}$ is given in Eq. (12).

The next theorem establishes the stability of the closed-loop reference system in Eq. (18).

Theorem 1: If the controller gains k_1, k_2, and the low-pass filter in the estimator are chosen to verify

$$k_2 > \frac{8(M_{\rho_r} + M_d(k_1))M_{\beta_{1r}}}{L_{\beta_{1r}}(1 - \epsilon)}, \qquad k_2 > k_1 \tag{23a}$$

$$\|1 - C(s)\|_{\mathcal{L}_1} < \frac{L_{\beta_{1r}}(1 - \epsilon)}{8M_t(M_{\beta_1}\mu_{\beta_2} + \mu_{\beta_1})} \tag{23b}$$

the initial conditions $\omega_r(0)$, $\rho_r(0)$, $\eta_r(0)$ and the reference ρ_d comply with

$$\|\omega_r(0) - \omega_0\|_\infty < \frac{L_{\beta_1 r}(1 - \epsilon)}{4(M_{\beta_1}\mu_{\beta_2} + \mu_{\beta_1})} \tag{24a}$$

$$|\rho_r(0) - \rho_d| < \frac{L_{\beta_1 r}(1 - \epsilon)}{k_1} - \underbrace{\left[\frac{(M_{\rho_r} + M_d(k_1))M_{\beta_{1r}}}{k_1 k_2} + \frac{(M_{\beta_1}\mu_{\beta_2} + \mu_{\beta_1})(\gamma_{c\omega} + \|\hat{\omega}_0 - \omega_0\|_\infty)}{k_1}\right]}_{B_0} \tag{24b}$$

$$|\eta_r(0) - \eta_d(\omega_r(0), \rho_r(0))| < \frac{k_1}{M_{\beta_{1r}}}|\rho_r(0) - \rho_d| \tag{24c}$$

$$B_0 + \gamma_b < \rho_r(0) \tag{24d}$$

and

$$\rho_d \geq \underbrace{|\rho_r(0) - \rho_d| + B_0}_{\bar{\gamma}_{r_1}} + \gamma_b \tag{25}$$

The closed-loop reference system in Eq. (18) is uniformly ultimately bounded. Moreover,

$$|\rho_r(t) - \rho_d| < \gamma_{r_1}(t) < \frac{L_{\beta_1 r}}{k_1}(1-\epsilon) \tag{26a}$$

$$|\eta_r(t) - \eta_d(\omega_r(t), \rho_r(t))| < \gamma_{r_2}(t) \tag{26b}$$

with

$$\begin{aligned}\gamma_{r_1}(t) &= |\rho_r(0) - \rho_d| e^{-k_1 t} + \frac{M_{\beta_{1r}} |\eta_r(0) - \eta_d(\omega_r(0), \rho_r(0))|}{k_1 - k_2} \\ &\times (e^{-k_2 t} - e^{-k_1 t}) + \frac{M_{\beta_1}\mu_{\beta_2} + \mu_{\beta_1}}{k_1} \|\omega_0 - \hat{\omega}_0\|_\infty e^{-ct} \\ &+ \underbrace{\frac{(M_{\rho_r} + M_d(k_1))M_{\beta_{1r}}}{k_1 k_2} + \frac{(M_{\beta_1}\mu_{\beta_2} + \mu_{\beta_1})\gamma_{c\omega}}{k_1}}_{B_\rho}\end{aligned} \tag{27a}$$

$$\gamma_{r_2}(t) = |\eta_r(0) - \eta_d(\omega_r(0), \rho_r(0))| e^{-k_2 t} + \underbrace{\frac{M_{\rho_r} + M_d(k_1)}{k_2}}_{B_\eta} \tag{27b}$$

Proof: It is straightforward to check that conditions (23) and (24a) ensure that the right-hand side of inequality (24b) is greater than $L_{\beta_{1r}}(1-\epsilon)/(2k_1)$ (Appendix C). As a result, inequalities (24b) and (24c) can be valid. It is shown in Appendix D that inequalities (23a) and (24c) lead to

$$\gamma_{r_1}(t) \leq \bar{\gamma}_{r_1} \tag{28}$$

where $\bar{\gamma}_{r_1}$ is given in Eq. (25). It follows from inequalities (24b) and (28) that

$$\gamma_{r_1}(t) < \frac{L_{\beta_1 r}}{k_1}(1-\epsilon) \tag{29}$$

Thus, to prove inequality (26a), it remains to show

$$|\rho_r(t) - \rho_d| < \gamma_{r_1}(t) \tag{30}$$

$$\begin{aligned}|f(0)| &= \left|\frac{-k_1(\rho_r(0) - \rho_d)}{\beta_1(\omega_r(0))}\right| < \frac{k_1}{|\beta_1(\omega_r(0))|}\frac{L_{\beta_1 r}}{k_1}(1-\epsilon) \\ &< \frac{L_{\beta_1 r}}{|\beta_1(\omega_r(0))|}(1-\epsilon) < 1-\epsilon\end{aligned} \tag{32}$$

If inequality (31) is not true for all $t \geq 0$, since $f(t)$ is continuous and $|f(0)| < 1-\epsilon$, there exists τ_u such that

$$|f(t)| \leq 1-\epsilon, \qquad t \in [0, \tau_u] \tag{33a}$$

$$|f(\tau_u)| = 1-\epsilon \tag{33b}$$

It then follows from Eqs. (21) and (33a) that $\dot{\eta}_d(\omega_r(t), \rho_r(t))$ is bounded over $[0, \tau_u]$. Thus, $M_d(k_1)$ in Eq. (22a) exists.

If $|\rho_r(t) - \rho_d| < \gamma_{r_1}(t)$ is not true, since

$$|\rho_r(0) - \rho_d| < \gamma_{r_1}(t) \tag{34}$$

and $\rho_r(t)$ is continuous, there exists τ such that

$$|\rho_r(t) - \rho_d| \leq \gamma_{r_1}(t), \qquad t \in [0, \tau] \tag{35a}$$

$$|\rho_r(\tau) - \rho_d| = \gamma_{r_1}(\tau) \tag{35b}$$

Before continuing with the proof, let us clarify the relationship between τ and τ_u. It follows from Eq. (33b) that

$$\begin{aligned}|f(\tau_u)| &= \left|\frac{-k_1(\rho_r(\tau_u) - \rho_d)}{\beta_1(\omega_r(\tau_u))}\right| \\ &= 1-\epsilon \Rightarrow |\rho_r(\tau_u) - \rho_d| \\ &= \frac{|\beta_1(\omega_r(\tau_u))|}{k_1}(1-\epsilon) \geq \frac{L_{\beta_{1r}}}{k_1}(1-\epsilon) > \gamma_{r_1}(t)\end{aligned}$$

Therefore, $\tau < \tau_u$.

It follows from Eq. (35a) that

$$\rho_d - \gamma_{r_1}(t) \leq \rho_r(t) \leq \rho_d + \gamma_{r_1}(t), \quad \forall\ t \in [0, \tau]$$

Then choosing ρ_d according to Eq. (25) leads to

$$\rho_r(t) \geq \gamma_b \tag{36}$$

Thus, M_{ρ_r} in Eq. (22b) exists. Note that such selection of ρ_d is feasible, as shown in Appendix E.

Considering $\dot{\eta}_r(t) - \dot{\eta}_d(\omega_r(t), \rho_r(t))$, it follows from the dynamics of $\eta_r(t)$ in Eq. (18) that

$$\begin{aligned}\dot{\eta}_r(t) - \dot{\eta}_d(\omega_r(t), \rho_r(t)) &= -k_2(\eta_r(t) - \eta_d(\omega_r(t), \rho_r(t))) \\ &+ \underbrace{\frac{V_t(t)\cos(\psi_t(t) - (\psi(t) - \eta_r(t))) - V_r(t)\cos(\psi_r(t) - (\psi(t) - \eta_r(t)))}{\rho_r(t)} - \dot{\eta}_d(\omega_r(t), \rho_r(t))}_{\delta_{r_1}(t)}\end{aligned} \tag{37}$$

First, contradiction is used to show that

$$\left|\underbrace{\frac{-k_1(\rho_r(t) - \rho_d)}{\beta_1(\omega_r(t))}}_{f(t)}\right| < 1-\epsilon \tag{31}$$

along the system trajectories in Eq. (18) subject to conditions (24). Considering $|f(0)|$, it follows from Eq. (24b) and the definition of $L_{\beta_1 r}$ in Eq. (22c) that

Summarizing the above, it follows from Eqs. (22), (33a), (36), and (37) that $\delta_{r_1}(t)$ is bounded by

$$|\delta_{r_1}(t)| < M_{\rho_r} + M_d(k_1) \tag{38}$$

Note that $\eta_r(t)$ can be decomposed into two components:

$$\eta_r(t) = \eta_{r_1}(t) + \eta_{r_2}(t) \tag{39}$$

where $\eta_{r_1}(t)$ and $\eta_{r_2}(t)$ are defined via

$$\dot{\eta}_{r_1}(t) - \tfrac{1}{2}\dot{\eta}_d(\omega_r(t), \rho_r(t)) = -k_2(\eta_{r_1}(t) - \tfrac{1}{2}\eta_d(\omega_r(t), \rho_r(t)))$$
$$\eta_{r_1}(0) = \eta_r(0) - \tfrac{1}{2}\eta_d(\omega_r(0), \rho_r(0)) \tag{40a}$$

$$\dot{\eta}_{r_2}(t) - \tfrac{1}{2}\dot{\eta}_d(\omega_r(t), \rho_r(t)) = -k_2(\eta_{r_2}(t) - \tfrac{1}{2}\eta_d(\omega_r(t), \rho_r(t))) + \delta_{r_1}(t)$$
$$\eta_{r_2}(0) = \tfrac{1}{2}\eta_d(\omega_r(0), \rho_r(0)) \tag{40b}$$

It follows from Eq. (40a) that

$$\eta_{r_1}(t) - \tfrac{1}{2}\eta_d(\omega_r(t), \quad \rho_r(t)) = (\eta_r(0) - \eta_d(\omega_r(0), \rho_r(0)))e^{-k_2 t} \tag{41}$$

It follows from Eqs. (38) and (40b), and Lemma 1 (see Appendix B) that

$$\left|\eta_{r_2}(t) - \frac{1}{2}\eta_d(\omega_r(t), \rho_r(t))\right| < \frac{M_{\rho_r} + M_d(k_1)}{k_2} \tag{42}$$

Equation (41), together with inequality (42), leads to

$$|\eta_r(t) - \eta_d(\omega_r(t), \rho_r(t))| < |\eta_r(0) - \eta_d(\omega_r(0), \rho_r(0))|e^{-k_2 t} + \frac{M_{\rho_r} + M_d(k_1)}{k_2} \tag{43}$$

which proves relationship (26b).

It follows from the dynamics of $\rho_r(t)$ in Eq. (18) that

$$\begin{aligned}\dot{\rho}_r(t) &= -k_1(\rho_r(t) - \rho_d) + \beta_1(\omega(t))\sin(\eta_r(t) + \beta_2(\omega(t))) \\ &\quad - \beta_1(\omega_r(t))\sin(\eta_d(\omega_r(t), \rho_r(t)) + \beta_2(\omega_r(t))) \\ &= -k_1(\rho_r(t) - \rho_d) + \delta_{r_2}(t) + \delta_{r_3}(t) \\ \delta_{r_2}(t) &= \beta_1(\omega_r(t))\sin(\eta_r(t) + \beta_2(\omega_r(t))) \\ &\quad - \beta_1(\omega_r(t))\sin(\eta_r(t) + \beta_2(\omega_r(t))) \\ \delta_{r_3}(t) &= \beta_1(\omega_r(t))\sin(\eta_r(t) + \beta_2(\omega_r(t))) \\ &\quad - \beta_1(\omega_r(t))\sin(\eta_d(\omega_r(t), \rho_r(t)) + \beta_2(\omega_r(t)))\end{aligned} \tag{44}$$

where

$$\begin{aligned}|\delta_{r_2}(t)| &= |\beta_1(\omega(t))\sin(\eta_r(t) + \beta_2(\omega(t))) \\ &\quad - \beta_1(\omega_r(t))\sin(\eta_r(t) + \beta_2(\omega_r(t)))| \\ &\le |\beta_1(\omega(t))\sin(\eta_r(t) + \beta_2(\omega(t))) - \beta_1(\omega(t))\sin(\eta_r(t) \\ &\quad + \beta_2(\omega_r(t)))| + |\beta_1(\omega(t))\sin(\eta_r(t) + \beta_2(\omega_r(t))) \\ &\quad - \beta_1(\omega_r(t))\sin(\eta_r(t) + \beta_2(\omega_r(t)))| \\ &\le |\beta_1(\omega(t))||\sin(\eta_r(t) + \beta_2(\omega(t))) \\ &\quad - \sin(\eta_r(t) + \beta_2(\omega_r(t)))| + |\beta_1(\omega(t)) - \beta_1(\omega_r(t))|\end{aligned} \tag{45}$$

It follows from inequalities (22c) and (45) that

$$|\delta_{r_2}(t)| < (M_{\beta_1}\mu_{\beta_2} + \mu_{\beta_1})\|\omega(t) - \omega_r(t)\|_\infty, \quad \forall\ t \ge 0 \tag{46}$$

Considering $\delta_{r_3}(t)$ in Eq. (44), it follows from Eq. (43) that

$$|\delta_{r_3}(t)| < |\beta_1(\omega_r(t))||\eta_r(t) - \eta_d(\omega_r(t), \rho_r(t))| < |\beta_1(\omega_r(t))| \times \left|(\eta_r(0) - \eta_d(\omega_r(0), \rho_r(0)))e^{-k_2 t} + \frac{M_{\rho_r} + M_d(k_1)}{k_2}\right| \tag{47}$$

It follows from inequalities (22c), (46), and (47) that for all $t \ge 0$,

$$|\delta_{r_2}(t) + \delta_{r_3}(t)| < M_{\beta_{1r}}|\eta_r(0) - \eta_d(\omega_r(0), \rho_r(0))|e^{-k_2 t} + \frac{M_{\beta_{1r}}(M_{\rho_r} + M_d(k_1))}{k_2} + (M_{\beta_1}\mu_{\beta_2} + \mu_{\beta_1})\|\omega(t) - \omega_r(t)\|_\infty \tag{48}$$

Note that $\rho_r(t)$ can be decomposed into two components:

$$\rho_r(t) = \rho_{r_1}(t) + \rho_{r_2}(t) \tag{49}$$

where $\rho_{r_1}(t)$ and $\rho_{r_2}(t)$ are defined via

$$\dot{\rho}_{r_1}(t) = -k_1\left(\rho_{r_1}(t) - \frac{\rho_d}{2}\right), \qquad \rho_{r_1}(0) = \rho_r(0) - \frac{\rho_d}{2} \tag{50a}$$

$$\dot{\rho}_{r_2}(t) = -k_1\left(\rho_{r_2}(t) - \frac{\rho_d}{2}\right) + \delta_{r_2}(t) + \delta_{r_3}(t), \qquad \rho_{r_2}(0) = \frac{\rho_d}{2} \tag{50b}$$

It follows from Eq. (50a) that

$$\rho_{r_1}(t) - \frac{\rho_d}{2} = (\rho_r(0) - \rho_d)e^{-k_1 t} \tag{51}$$

To study the behavior of Eq. (50b), first consider the following scalar linear time-varying system

$$\dot{x}(t) = -\bar{k}_1 x(t) + \delta(t), \qquad x(0) = 0 \tag{52}$$

with

$$|\delta(t)| < \bar{M}e^{-\bar{k}_2 t} \tag{53}$$

where $\bar{k}_1, \bar{k}_2$, and $\bar{M}$ are positive constants. For the system in Eq. (52) subject to inequality (53), one can obtain

$$\begin{aligned}|x(t)| &= \left|\int_0^t e^{-\bar{k}_1(t-\tau)}\delta(\tau)\,\mathrm{d}\tau\right| < \int_0^t e^{-\bar{k}_1(t-\tau)}|\delta(\tau)|\,\mathrm{d}\tau \\ &< \int_0^t e^{-\bar{k}_1(t-\tau)}\bar{M}e^{-\bar{k}_2\tau}\,\mathrm{d}\tau < \frac{\bar{M}}{\bar{k}_1 - \bar{k}_2}(e^{-\bar{k}_2 t} - e^{-\bar{k}_1 t})\end{aligned} \tag{54}$$

It follows from inequalities (48) and (54) and Lemma 1 that

$$\left|\rho_{r_2}(t) - \frac{\rho_d}{2}\right| < \frac{M_{\beta_{1r}}|\eta_r(0) - \eta_d(\omega_r(0), \rho_r(0))|}{k_1 - k_2}(e^{-k_2 t} - e^{-k_1 t}) + \frac{(M_{\rho_r} + M_d(k_1))M_{\beta_{1r}}/k_2 + (M_{\beta_1}\mu_{\beta_2} + \mu_{\beta_1})\|\omega(t) - \omega_r(t)\|_\infty}{k_1}, \quad \forall\ t \ge 0 \tag{55}$$

Equation (51), along with inequalities (16) and (55), leads to

$$|\rho_r(t) - \rho_d| < \gamma_{r_1}(t)$$

which contradicts Eq. (35b). Therefore, relationship (30) holds. Finally, it follows from inequalities (29) and (30) that relationship (26a) holds over $[0, \tau_u]$.

Accordingly, for $t \in [0, \tau_u]$,

$$\begin{aligned}|f(t)| &= \left|\frac{-k_1(\rho_r(t) - \rho_d)}{\beta_1(\omega_r(t))}\right| < \frac{k_1\gamma_{r_1}(t)}{|\beta_1(\omega_r(t))|} \\ &< \frac{k_1}{|\beta_1(\omega_r(t))|}\frac{L_{\beta_{1r}}}{k_1}(1 - \epsilon) < 1 - \epsilon\end{aligned} \tag{56}$$

which contradicts Eq. (33b). Therefore, inequality (31) holds along the system trajectories in Eq. (18) subject to conditions (24) for all $t \ge 0$. This completes the proof. □

Remark 1: [Conditions (24)*]*

1) Condition (24b) ensures that $|f(t)| < 1 - \epsilon$ so that $\sin^{-1}(f(t))$ is well-defined.

2) Condition (24c), along with the selection of design gains $k_2 > k_1$ in condition (23a), ensures that the tracking performance bound of $\rho_r(t) - \rho_d$ decreases monotonically per the upper bound given in Eq. (27a) for all $t \ge 0$.

3) Since $\rho_r(t)$ appears in the denominator of Eq. (18), $\rho_r(t)$ needs to be regulated to be bounded away from zero. Selection of ρ_d in condition (25) helps to achieve this objective. Condition (24d) ensures that such selection of ρ_d is feasible.

B. Region of Attraction of the Closed-Loop Reference System

Let

$$\tilde{\mathcal{X}}_0 = [\tilde{\omega}_0, \tilde{\rho}_0, \tilde{\eta}_0]^\top \qquad \tilde{\omega}_0 = \omega_r(0) - \omega_0 = \hat{\omega}_0 - \omega_0$$
$$\tilde{\rho}_0 = \rho_r(0) - \rho_d = \rho_0 - \rho_d \tag{57}$$
$$\tilde{\eta}_0 = \eta_r(0) - \eta_d(\omega_r(0), \rho_r(0)) = \eta_0 - \eta_d(\hat{\omega}_0, \rho_0)$$

Inequalities (24a–24c) can be rewritten as

$$\|\tilde{\omega}_0\|_\infty < \underbrace{\frac{L_{\beta_{1r}}(1-\epsilon)}{4(M_{\beta_1}\mu_{\beta_2} + \mu_{\beta_1})}}_{B_{\tilde{\omega}_0}}, \qquad |\tilde{\rho}_0| < \underbrace{\frac{L_{\beta_{1r}}(1-\epsilon)}{k_1} - B_0}_{B_{\tilde{\rho}_0}}$$
$$|\tilde{\eta}_0| < \frac{k_1}{M_{\beta_1 r}}|\tilde{\rho}_0| < \underbrace{\frac{k_1}{M_{\beta_1 r}} B_{\tilde{\rho}_0}}_{B_{\tilde{\eta}_0}} \tag{58}$$

From Eqs. (27a) and (58), it is possible to conclude that for the choice of k_1, k_2, and $C(s)$ in Eq. (23), and the choice of ρ_d in Eq. (25), the domain given by

$$\Omega_r = \{(\tilde{\omega}_0, \tilde{\rho}_0, \tilde{\eta}_0)\colon \|\tilde{\omega}_0\|_\infty < B_{\tilde{\omega}_0}, |\tilde{\rho}_0| < B_{\tilde{\rho}_0}, |\tilde{\eta}_0| < B_{\tilde{\eta}_0}\} \tag{59}$$

is the region of attraction of the reference system in Eq. (18) with ultimate bound B_ρ. Decreasing k_1 enlarges the region of attraction at the cost of larger ultimate bound B_ρ. Note that conditions (23) and (24a) ensure that

$$B_\rho = \frac{(M_{\rho_r} + M_d(k_1))M_{\beta_{1r}}}{k_1 k_2} + \frac{(M_{\beta_1}\mu_{\beta_2} + \mu_{\beta_1})\gamma_{c\omega}}{k_1}$$
$$< \frac{L_{\beta_{1r}}(1-\epsilon)}{4k_1} < B_{\tilde{\rho}_0} \tag{60a}$$

$$B_\eta = \frac{M_{\rho_r} + M_d(k_1)}{k_2} < \frac{L_{\beta_{1r}}(1-\epsilon)}{8M_{\beta_{1r}}} < B_{\tilde{\eta}_0} \tag{60b}$$

The two inequalities (60) will be used in Sec. IV.D to establish the arbitrary closeness between the reference system in Eq. (18) and the adaptive system to be presented next.

C. Adaptive System

Theorem 1 characterizes both the transient and the steady-state performance of the reference system (18). In this section, it is shown that the trajectories of the closed-loop adaptive system can stay arbitrarily close to this reference system.

The closed-loop adaptive system, defined by application of the controller in Eq. (17) to the system in Eq. (1), can be written as

$$\begin{cases} \dot{\rho}(t) = \beta_1(\omega(t))\sin(\eta(t) + \beta_2(\omega(t))),\ \rho(0) = \rho_0 \\ \dot{\eta}(t) = -\frac{V_g(t)\cos\eta(t) - V_t(t)\cos[\psi_t(t) - (\psi(t) - \eta(t))]}{\rho(t)} + \dot{\psi}(t),\ \eta(0) = \eta_0 \\ \dot{\psi}(t) = \frac{V_g(t)\cos\eta(t) - \hat{V}_t(t)\cos[\hat{\psi}_t(t) - (\psi(t) - \eta(t))]}{\rho(t)} - k_2(\eta(t) - \eta_d(\omega_e(t), \rho(t))) \\ \eta_d(\omega_e(t), \rho(t)) = \sin^{-1}\left(\frac{-k_1(\rho(t) - \rho_d)}{\beta_1(\omega_e(t))}\right) - \beta_2(\omega_e(t)) \end{cases} \tag{61}$$

where $\omega_e(t)$ is given in Eq. (9b). Note that $\omega_e(t)$, $\hat{V}_t(t)$, and $\hat{\psi}_t(t)$ are all bounded signals.

D. Transient and Steady-State Performance

Let

$$\tilde{\rho}(t) = \rho(t) - \rho_r(t), \qquad \tilde{\eta}(t) = \eta(t) - \eta_r(t) \tag{62}$$

The error dynamics between Eqs. (18) and (61) can be written as

$$\dot{\tilde{\rho}}(t) = \beta_1(\omega(t))\sin(\eta(t) + \beta_2(\omega(t)))$$
$$- \beta_1(\omega(t))\sin(\eta_r(t) + \beta_2(\omega(t)))$$
$$= -k_1(\rho(t) - \rho_d) + \beta_1(\omega(t))\sin(\eta(t) + \beta_2(\omega(t)))$$
$$- \beta_1(\omega_e(t))\sin(\eta_d(\omega_e(t), \rho(t)) + \beta_2(\omega_e(t)))$$
$$+ k_1(\rho_r(t) - \rho_d) - \beta_1(\omega(t))\sin(\eta_r(t) + \beta_2(\omega(t)))$$
$$+ \beta_1(\omega_r(t))\sin(\eta_d(\omega_r(t), \rho_r(t)) + \beta_2(\omega_r(t)))$$
$$= -k_1(\rho(t) - \rho_r(t)) + \beta_1(\omega(t))[\sin(\eta(t) + \beta_2(\omega(t)))$$
$$- \sin(\eta_r(t) + \beta_2(\omega(t)))] + \beta_1(\omega_r(t))\sin(\eta_d(\omega_r(t), \rho_r(t))$$
$$+ \beta_2(\omega_r(t))) - \beta_1(\omega_e(t))\sin(\eta_d(\omega_e(t), \rho(t)) + \beta_2(\omega_e(t))) \tag{63a}$$

$$\dot{\tilde{\eta}}(t) = -k_2(\eta(t) - \eta_r(t)) + k_2[\eta_d(\omega_e(t), \rho(t)) - \eta_d(\omega_r(t), \rho_r(t))]$$
$$+ [V_t(t)\cos(\psi_t(t) - \psi(t) + \eta(t)) - \hat{V}_t(t)\cos(\hat{\psi}_t(t)$$
$$- \psi(t) + \eta(t))]/\rho(t) - [V_t(t)\cos(\psi_t(t) - \psi(t) + \eta_r(t))$$
$$- V_r(t)\cos(\psi_r(t) - \psi(t) + \eta_r(t))]/\rho_r(t) \tag{63b}$$

Next, consider boundedness of the signals that will be used in establishing the stability of the closed-loop adaptive system in Eq. (61). Since the function $\beta_1(t)$ is continuous, there exist finite constants $L_{\beta_{1e}}$ and μ_e such that for $\forall\ t \geq 0$,

$$L_{\beta_{1e}} < |\beta_1(\omega_e(t))|, \qquad \left|\frac{\beta_1(\omega_r(t))}{\beta_1(\omega_e(t))}\right| \leq \mu_e\|\omega_e(t) - \omega_r(t)\|_\infty \tag{64a}$$

If $|k_1(\rho(t) - \rho_d)/\beta_1(\omega_e(t))| \leq 1 - \epsilon$ and $\tilde{\mathcal{X}}_0 \in \Omega_r$, there exist finite L_1 and L_2 such that

$$|\eta_d(\omega_e(t), \rho(t)) - \eta_d(\omega_r(t), \rho_r(t))| < L_1\|\omega_e(t) - \omega_r(t)\|_\infty$$
$$+ L_2|\rho(t) - \rho_r(t)|, \quad \forall\ t \geq 0 \tag{64b}$$

Further, if $\rho(t) \geq \bar{\gamma}_b$, where $\bar{\gamma}_b$ is a positive constant, there exist finite constants μ_ρ, M_{ρ_1}, and M_{ρ_2} such that for all $t \geq 0$,

$$\left|\frac{2\hat{V}_t(t)(\hat{\psi}_t(t) - \psi_r(t)) + (\hat{V}_t(t) - V_r(t))}{\rho(t)}\right| \leq \mu_\rho\|\omega_e(t) - \omega_r(t)\|_\infty$$
$$\left|\frac{2V_t(t)\hat{V}_t(t)}{\rho(t)}\right| \leq M_{\rho_1}, \qquad \left|\frac{V_t(t)\hat{V}_t(t)}{\rho(t)\rho_r(t)}\right| \leq M_{\rho_2} \tag{64c}$$

It is proved in Appendix F that when inequalities (64b) and (64c) hold with finite constants L_1, L_2, μ_ρ, M_{ρ_1}, and M_{ρ_2}, the error dynamics in Eq. (63) can be written as

$$\dot{\tilde{\rho}}(t) = -k_1\tilde{\rho}(t) + \Delta_\rho(t) \tag{65a}$$

$$\dot{\tilde{\eta}}(t) = -k_2\tilde{\eta}(t) + \Delta_\eta(t) \tag{65b}$$

where definitions of $\Delta_\rho(t)$ and $\Delta_\eta(t)$ follow from Eq. (63). In Eq. (65), for all $t \geq 0$,

$$|\Delta_\rho(t)| \leq \kappa_1|\tilde{\rho}(t)| + \kappa_2|\tilde{\eta}(t)| + \kappa_3\|\omega_e(t) - \omega_r(t)\|_\infty \tag{66a}$$

$$|\Delta_\eta(t)| \leq \kappa_4|\tilde{\eta}(t)| + \kappa_5|\tilde{\rho}(t)| + \kappa_6\|\omega_e(t) - \omega_r(t)\|_\infty \tag{66b}$$

where κ_i for $i = 1, \ldots, 6$ are positive constants chosen as

$$\kappa_1 = M_{\beta_1 r}L_2$$
$$\kappa_2 = M_{\beta_1}$$
$$\kappa_3 = M_{\beta_{1r}} + M_{\beta_1 r}\mu_{\beta_2} + \mu_{\beta_1}$$
$$\kappa_4 = M_{\rho_1}$$
$$\kappa_5 = M_{\rho_2} + k_2L_2$$
$$\kappa_6 = \mu_\rho + k_2L_1 \tag{67}$$

with M_{β_1}, $M_{\beta_{1r}}$, μ_{β_1}, and μ_{β_2} given in Eq. (22c); L_1 and L_2 given in Eq. (64b); and μ_ρ, M_{ρ_1}, and M_{ρ_2} given in Eq. (64c).

Let

$$a_{\rho_l} = k_1 - \kappa_1 - \epsilon_{k_1}, \qquad a_{\eta_l} = k_2 - \kappa_4 - \epsilon_{k_2} \tag{68}$$

where ϵ_{k_1} and ϵ_{k_2} are positive numbers. The following theorem states the transient and steady-state performance of the adaptive system in Eq. (61).

Theorem 2: Consider the closed-loop reference system in Eq. (18), subject to conditions (23–25), and the closed-loop adaptive system in Eq. (61). If the controller gains k_1 and k_2 and the adaptation gain Γ_c in the estimator are chosen as

$$a_{\rho_l} a_{\eta_l} - \kappa_2\kappa_5 > 0 \tag{69a}$$

$$\sqrt{\Gamma_c} > \gamma_c \max\left\{\frac{1}{B_{\tilde{\omega}_0}}, \frac{2(K_\rho+\epsilon_\rho)}{B_{\tilde{\rho}_0}-B_\rho}, \frac{2(K_\eta+\epsilon_\eta)+L_1+L_2(K_\rho+\epsilon_\rho)}{B_{\tilde{\eta}_0}-B_\eta}, \times\frac{k_1(K_\rho+\epsilon_\rho)}{L_{\beta_{1e}}(1-\epsilon)}+\mu_e, \frac{K_\rho+\epsilon_\rho}{\gamma_b-\bar{\gamma}_b}\right\} \tag{69b}$$

and the initial values $\omega_e(0)$, $\rho(0)$, and $\eta(0)$ comply with

$$\|\omega_e(0)-\omega_0\|_\infty = \|\hat{\omega}_0-\omega_0\|_\infty < B_{\tilde{\omega}_0} - \gamma_0 \tag{70a}$$

$$|\rho(0)-\rho_d| = |\rho_0-\rho_d| < B_{\tilde{\rho}_0} - \gamma_\rho \tag{70b}$$

$$|\eta(0)-\eta_d(\omega_e(0),\rho(0))| = |\eta_0-\eta_d(\hat{\omega}_0,\rho_0)| < B_{\tilde{\eta}_0} - \gamma_\eta \tag{70c}$$

one can have

$$\|\omega_e-\omega_r\|_{\mathcal{L}_\infty} \le \gamma_0 \tag{71a}$$

$$\|\rho-\rho_r\|_{\mathcal{L}_\infty} < \gamma_\rho \tag{71b}$$

$$\|\eta-\eta_r\|_{\mathcal{L}_\infty} < \gamma_\eta \tag{71c}$$

where

$$\gamma_0 = \frac{\gamma_c}{\sqrt{\Gamma_c}} \tag{72a}$$

$$\gamma_\rho = (K_\rho+\epsilon_\rho)\gamma_0 \tag{72b}$$

$$\gamma_\eta = (K_\eta+\epsilon_\eta)\gamma_0 \tag{72c}$$

$$K_\rho = \frac{\kappa_2\kappa_6+\kappa_3 a_{\eta_l}}{a_{\rho_l}a_{\eta_l}-\kappa_2\kappa_5} \tag{72d}$$

$$K_\eta = \frac{\kappa_3\kappa_5+a_{\rho_l}\kappa_6}{a_{\rho_l}a_{\eta_l}-\kappa_2\kappa_5} \tag{72e}$$

and ϵ_ρ and ϵ_η are positive constants; κ_i (for $i = 1,\ldots,6$) are given in Eq. (67); a_{ρ_l} and a_{η_l} are given in Eq. (68); $\gamma_b > \bar{\gamma}_b > 0$, $B_{\tilde{\omega}_0}$, $B_{\tilde{\rho}_0}$, and $B_{\tilde{\eta}_0}$ are given in Eq. (58); and γ_c is given in Eq. (13).

Proof: It is straightforward to check that the selection of Γ_c in Eq. (69b) ensures that the right-hand sides of inequalities (70) are greater than 0 so that Eq. (70) holds (Appendix G). Inequality (71a) follows from Eq. (12) immediately. Inequalities (71b) and (71c) will be proved by contradiction.

Since $\eta(t)$, $\eta_r(t)$, $\rho(t)$, and $\rho_r(t)$ are continuous and

$$|\rho(0)-\rho_r(0)| = 0 \le \gamma_\rho, \qquad |\eta(0)-\eta_r(0)| = 0 \le \gamma_\eta \tag{73}$$

if relationships (71b) and (71c) are not true, there exists $\tau > 0$ such that

$$|\rho(\tau)-\rho_r(\tau)| = \gamma_\rho, \quad \text{or} \quad |\eta(\tau)-\eta_r(\tau)| = \gamma_\eta \tag{74}$$

while

$$\|(\rho-\rho_r)_\tau\|_{\mathcal{L}_\infty} \le \gamma_\rho, \qquad \|(\eta-\eta_r)_\tau\|_{\mathcal{L}_\infty} \le \gamma_\eta \tag{75}$$

Here, $\|(\cdot)_\tau\|_{\mathcal{L}_\infty}$ denotes the truncated $\mathcal{L}_\infty$-norm, whose definition is given in Equation (A1).

In the following, it is shown that $|k_1(\rho(t)-\rho_d)/\beta_1(\omega_e(t))| < 1-\epsilon$ and $\rho(t) \ge \bar{\gamma}_b$ for $t \in [0,\tau]$. Considering $|k_1(\rho(t)-\rho_d)/\beta_1(\omega_e(t))|$, one can obtain

$$\begin{aligned}
\left|\frac{k_1(\rho(t)-\rho_d)}{\beta_1(\omega_e(t))}\right| &\le \left|\frac{k_1(\rho(t)-\rho_r(t))}{\beta_1(\omega_e(t))}\right| + \left|\frac{k_1(\rho_r(t)-\rho_d)}{\beta_1(\omega_e(t))}\right| \\
&\le \frac{k_1}{|\beta_1(\omega_e(t))|}\gamma_\rho + \frac{k_1}{|\beta_1(\omega_e(t))|}\frac{L_{\beta_{1r}}(1-\epsilon)}{k_1} \\
&= \frac{k_1}{|\beta_1(\omega_e(t))|}(K_\rho+\epsilon_\rho)\gamma_0 + \frac{L_{\beta_{1r}}}{|\beta_1(\omega_r(t))|}\left|\frac{\beta_1(\omega_r(t))}{\beta_1(\omega_e(t))}\right|(1-\epsilon) \\
&\le \frac{k_1}{|\beta_1(\omega_e(t))|}(K_\rho+\epsilon_\rho)\gamma_0 + \left|\frac{\beta_1(\omega_r(t))}{\beta_1(\omega_e(t))}\right|(1-\epsilon) \\
&\le \left(\frac{k_1(K_\rho+\epsilon_\rho)}{L_{\beta_{1e}}}+\mu_e(1-\epsilon)\right)\gamma_0 < 1-\epsilon
\end{aligned} \tag{76}$$

where relationships (22c), (26a), (64a), (69b), (71), and (75) have been used. Considering $\rho(t)$, it follows from Eq. (75) that

$$\rho_r(t)-\gamma_\rho \le \rho(t) \le \rho_r(t)+\gamma_\rho \quad \forall\ t \in [0,\tau] \tag{77}$$

The initial conditions (70), together with Eq. (75), ensure that $\tilde{\mathcal{X}}_0 \in \Omega_r$. Thus, for the reference system $\rho_r(t) \ge \gamma_b$ subject to Eqs. (23–25). It then follows from Eq. (77) and the selection of Γ_c in Eq. (69b) that $\rho(t) \ge \bar{\gamma}_b$ for $\gamma_b > \bar{\gamma}_b > 0$. Therefore, the finite constants L_1, L_2, μ_ρ, M_{ρ_1}, and M_{ρ_2} in Eq. (64) exist and Eqs. (65–68) hold.

Next, consider Eq. (65a). It follows from Eqs. (65a) and (66a) and Lemma 1 that

$$\|\tilde{\rho}_\tau\|_{\mathcal{L}_\infty} \le \frac{\kappa_2\|\tilde{\eta}_\tau\|_{\mathcal{L}_\infty}+\kappa_3\gamma_0}{a_{\rho_l}} \tag{78}$$

Similarly, it follows from Eqs. (65b) and (66b), and Lemma 1 that

$$\|\tilde{\eta}_\tau\|_{\mathcal{L}_\infty} \le \frac{\kappa_5\|\tilde{\rho}_\tau\|_{\mathcal{L}_\infty}+\kappa_6\gamma_0}{a_{\eta_l}} \tag{79}$$

Summarizing the above two inequalities leads to

$$\begin{aligned}
\|\tilde{\rho}_\tau\|_{\mathcal{L}_\infty} &\le \frac{\kappa_2}{a_{\rho_l}}\frac{\kappa_5\|\tilde{\rho}_\tau\|_{\mathcal{L}_\infty}+\kappa_6\gamma_0}{a_{\eta_l}} + \frac{\kappa_3}{a_{\rho_l}}\gamma_0 \\
&\le \frac{\kappa_2\kappa_5}{a_{\rho_l}a_{\eta_l}}\|\tilde{\rho}_\tau\|_{\mathcal{L}_\infty} + \left(\frac{\kappa_2\kappa_6}{a_{\rho_l}a_{\eta_l}}+\frac{\kappa_3}{a_{\rho_l}}\right)\gamma_0
\end{aligned} \tag{80}$$

Condition (69a) ensures that

$$\|\tilde{\rho}_\tau\|_{\mathcal{L}_\infty} \le \frac{\kappa_2\kappa_6+\kappa_3 a_{\eta_l}}{a_{\rho_l}a_{\eta_l}-\kappa_2\kappa_5}\gamma_0 \tag{81}$$

Similarly,

$$\|\tilde{\eta}_\tau\|_{\mathcal{L}_\infty} \le \frac{\kappa_3\kappa_5+a_{\rho_l}\kappa_6}{a_{\rho_l}a_{\eta_l}-\kappa_2\kappa_5}\gamma_0 \tag{82}$$

Thus,

$$\|\tilde{\rho}_\tau\|_{\mathcal{L}_\infty} \le K_\rho \gamma_0, \qquad \|\tilde{\eta}_\tau\|_{\mathcal{L}_\infty} \le K_\eta \gamma_0 \tag{83}$$

where K_ρ and K_η are given in Eq. (72). Inequality (83), together with the definitions of γ_ρ and γ_η in Eq. (72), implies that

$$\|\tilde{\rho}_\tau\|_{\mathcal{L}_\infty} < \gamma_\rho, \qquad \|\tilde{\eta}_\tau\|_{\mathcal{L}_\infty} < \gamma_\eta \tag{84}$$

which contradicts Eq. (74). Hence, relationships (71b) and (71c) must hold. This completes the proof. □

Remark 2: From Theorems 1 and 2, it is possible to conclude that for the choice of k_1, k_2, $C(s)$, and Γ_c in Eqs. (23) and (69), and the choice of ρ_d in Eq. (25),

$$\Omega = \{(\tilde{\omega}_0, \tilde{\rho}_0, \tilde{\eta}_0)\colon \|\tilde{\omega}_0\|_\infty < B_{\tilde{\omega}_0} - \gamma_0, |\tilde{\rho}_0| < B_{\tilde{\rho}_0} - \gamma_\rho, \; |\tilde{\eta}_0| < B_{\tilde{\eta}_0} - \gamma_\eta\} \tag{85}$$

is the region of attraction of the adaptive system in Eq. (61) with the ultimate bound $B_\rho + \gamma_\rho$.

Remark 3: [Conditions (69b)*]*

1) Condition $\sqrt{\Gamma_c} > \gamma_c / B_{\tilde{\omega}_0}$ ensures that the right-hand side of inequality (70a) is greater than 0 so that Eq. (70a) is valid.

2) Conditions

$$\sqrt{\Gamma_c} > \gamma_c \frac{2(K_\rho + \epsilon_\rho)}{B_{\tilde{\rho}_0} - B_\rho}$$

and

$$\sqrt{\Gamma_c} > \gamma_c \frac{2(K_\eta + \epsilon_\eta) + L_1 + L_2(K_\rho + \epsilon_\rho)}{B_{\tilde{\eta}_0} - B_\eta}$$

ensure that

$$\begin{gathered} B_\rho + \gamma_\rho < B_{\tilde{\rho}_0} - \gamma_\rho \\ B_\eta + \gamma_0[(K_\eta + \epsilon_\eta) + L_1 + L_2(K_\rho + \epsilon_\rho)] < B_{\tilde{\eta}_0} - \gamma_\eta \end{gathered} \tag{86}$$

which will be used in Sec. V when analyzing the system's stability in the presence of out-of-frame events.

3) Condition

$$\sqrt{\Gamma_c} > \gamma_c \frac{k_1(K_\rho + \epsilon_\rho)}{(L_{\beta_{1\epsilon}}(1-\epsilon)) + \mu_e}$$

ensures that

$$\left| \frac{k_1(\rho(t) - \rho_d)}{\beta_1(\omega_e(t))} \right| < 1 - \epsilon$$

for all $t \ge 0$ over Ω.

4) Condition $\sqrt{\Gamma_c} > \gamma_c(K_\rho + \epsilon_\rho)(\gamma_b - \bar{\gamma}_b)$ helps to ensure that $\rho(t) \ge \bar{\gamma}_b$ for all $t \ge 0$.

V. Stability in the Presence of Out-of-Frame Events

In vision-based applications, continuous extraction of the target's information is often unavailable due to environmental factors, limited field of view of the camera, or failure in the image-processing module. These phenomena are commonly referred to as out-of-frame events. The out-of-frame event cannot be avoided due to the complexity of a real application scenario. The problems due to temporary target loss need to be addressed explicitly.

For this purpose, the performance degradation of the closed-loop system is studied, casting it into the framework of switching systems. The switching system includes two subsystems, as shown in Fig. 2. One subsystem corresponds to the case when the visual measurements are available, and the other subsystem corresponds to the situation when the visual measurements are *not* available. The switching signal is the signal defining the out-of-frame event.

For the problem at hand, it is intuitive that stability of the subsystem in the presence of an out-of-frame event cannot be guaranteed. To characterize the stability of the closed-loop switched system, following [5], the concept of brief instabilities is exploited to model the out-of-frame events.

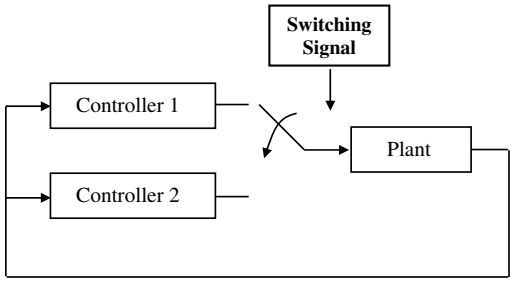

Fig. 2 Illustration of switching between two subsystems.

Define the tracking loss as a binary signal [3,5,24,25]:

$$s(t) := \begin{cases} 0 & \text{out-of-frame event at time } t, \\ 1 & \text{camera tracks the target at time } t \end{cases} \tag{87}$$

Following [5], let $T_s(\tau, t)$ denote the amount of time in the interval $[\tau, t]$ when $s(t) = 0$. Formally,

$$T_s(\tau, t) := \int_\tau^t (1 - s(t'))\, \mathrm{d}t'$$

We say that the image-processing experiences brief target loss if

$$T_s(\tau, t) \le T_0 + \alpha(t - \tau) \quad \forall\ t \ge \tau \ge 0 \tag{88}$$

for some $T_0 \ge 0$ and $\alpha \in [0, 1]$. The scalar T_0 is called the instability bound and α is called the asymptotic instability ratio ([5], page 891). Note that α provides an asymptotic upper bound on the ratio $T_s(\tau, t)/(t - \tau)$ as $(t - \tau) \to \infty$.

A. Estimator in the Presence of Out-of-Frame Events

When the target is out of frame, there are no measurement for $x(t) = [p_x(t), p_y(t)]^\top$. In this case, the guidance law uses the latest available estimate $\hat{\omega}(t)$ for the unknown parameters, treating it as constant. That is, referring to Eq. (8), let $\dot{\hat{\omega}}(t) = 0$ when $s(t) = 0$. Suppose that the measurements become available at time instant t_i. The initial state of $\hat{x}(t_i)$ is then set as $\hat{x}(t_i) = x(t_i)$. The state estimator and the update law in the presence of target loss become as shown next:

1) The state estimator is

$$\begin{gathered} \dot{\hat{x}}(t) = s(t) A_m \tilde{x}(t) - V_g(t) \begin{bmatrix} \sin\psi(t) \\ \cos\psi(t) \end{bmatrix} + \hat{\omega}(t) \\ \tilde{x}(t) = \hat{x}(t) - x(t) \end{gathered} \tag{89}$$

where $s(t)$ is defined in Eq. (87).

2) The update law is

$$\dot{\hat{\omega}}(t) = \Gamma_c \operatorname{Proj}(\hat{\omega}(t), -s(t) P^\top \tilde{x}(t)) \tag{90}$$

The low-pass filter in Eq. (10) and the extraction of unknown parameters in Eq. (11) remain the same.

B. Controller in the Presence of Out-of-Frame Events

In the controller design, note that the signals related to visual measurements become unavailable in the presence of target loss. Considering Eq. (17), these signals include $\rho(t)$, $\eta(t)$, and $\eta_d(\omega_e(t), \rho(t))$, which are therefore kept frozen during the out-of-frame time interval. In the presence of an out-of-frame event, the controller in Eq. (17) operates with frozen estimates:

$$\begin{cases} \dot{\psi}(t) = \frac{V_g(t)\cos\bar{\eta} - \bar{V}_t \cos[\bar{\psi}_t - (\psi(t) - \bar{\eta})]}{\bar{\rho}} - k_2(\bar{\eta} - \bar{\eta}_d), \\ \bar{\eta}_d = \sin^{-1}\left(\frac{-k_1(\bar{\rho} - \rho_d)}{\beta_1(\bar{V}_t, \bar{\psi}_t)}\right) - \beta_2(\bar{V}_t, \bar{\psi}_t) \end{cases} \tag{91}$$

where $\bar{V}_t$ is a constant, frozen from pervious estimate $\hat{V}_t(t)$; $\bar{\psi}_t$ is a constant, frozen from pervious estimate $\hat{\psi}_t(t)$; $\bar{\rho}$ is a constant, frozen from pervious quantity $\rho(t)$; $\bar{\eta}$ is a constant, frozen from pervious quantity $\eta(t)$; and $\bar{\eta}_d$ is a constant, frozen from pervious quantity $\eta_d(\omega_e(t), \rho(t))$.

C. Stability of Subsystems

There are two subsystems. One subsystem corresponds to the case when the visual measurements are available, referred to as $\mathcal{G}_1$ hereafter. The other subsystem, $\mathcal{G}_2$, corresponds to case of the out-of-frame event. The subsystem $\mathcal{G}_1$ is achieved by applying the controller in Eq. (17) to the plant in Eq. (1), using estimates in Eqs. (7–11) that are obtained from continuous visual measurements. The subsystem $\mathcal{G}_2$ is achieved via application of the controller in Eq. (91) to the plant, where signals related to visual measurements are kept frozen. These two subsystems are listed below:

Subsystem $\mathcal{G}_1$:

$$\begin{cases} \dot{\rho}(t) = \beta_1(V_t(t), \psi(t)) \sin(\eta(t) + \beta_2(V_t(t), \psi(t))) \\ \dot{\eta}(t) = -\frac{V_g(t)\cos\eta(t) - V_t(t)\cos[\psi_t(t) - (\psi(t) - \eta(t))]}{\rho(t)} \\ \qquad + \frac{V_g(t)\cos\eta(t) - \hat{V}_t(t)\cos[\hat{\psi}_t(t) - (\psi(t) - \eta(t))]}{\rho(t)} \\ \qquad - k_2(\eta(t) - \eta_d(\omega_e(t), \rho(t))) \end{cases} \tag{92}$$

where $\hat{V}_t(t)$ and $\hat{\psi}_t(t)$ are obtained through Eqs. (7–11).

Subsystem $\mathcal{G}_2$:

$$\begin{cases} \dot{\rho}(t) = \beta_1(V_t(t), \psi(t)) \sin(\eta(t) + \beta_2(V_t(t), \psi(t))) \\ \dot{\eta}(t) = -\frac{V_g(t)\cos\eta(t) - V_t(t)\cos[\psi_t(t) - (\psi(t) - \eta(t))]}{\rho(t)} \\ \qquad + \frac{V_g(t)\cos\bar{\eta} - \bar{V}_t\cos[\bar{\psi}_t - (\psi(t) - \bar{\eta})]}{\bar{\rho}} - k_2(\bar{\eta} - \bar{\eta}_d) \end{cases} \tag{93}$$

where $\bar{V}_t$, $\bar{\psi}_t$, $\bar{\rho}$, $\bar{\eta}$, and $\bar{\eta}_d$ are given in Eq. (91).

Considering $\mathcal{G}_1$, it has been shown in Theorems 1 and 2 that upon proper selection of the controller gains k_1 and k_2 per Eq. (69a) and the adaptation gain Γ_c per Eq. (69b), for $\tilde{\mathcal{X}}_0 \in \Omega$, the closed-loop system $\mathcal{G}_1$ can be designed to be arbitrarily close to the bounded reference system in Eq. (18). Let us consider $\lim_{t\to\infty}|\rho(t) - \rho_d|$. It follows from Eqs. (27a) and (71b) that

$$\lim_{t\to\infty}|\rho(t) - \rho_d| \le \lim_{t\to\infty}|\rho(t) - \rho_r(t)| + \lim_{t\to\infty}|\rho_r(t) - \rho_d| < B_\rho + \gamma_\rho \tag{94}$$

Similarly,

$$\begin{aligned} &\lim_{t\to\infty}|\eta(t) - \eta_d(\omega_e(t), \rho(t))| \\ &\quad = \lim_{t\to\infty}|[\eta(t) - \eta_r(t)] + [\eta_r(t) - \eta_d(\omega_r(t), \rho_r(t))]| \\ &\quad + \lim_{t\to\infty}|\eta_d(\omega_r(t), \rho_r(t)) - \eta_d(\omega_e(t), \rho(t))| \\ &\quad < \gamma_\eta + B_\eta + L_1\gamma_0 + L_2\gamma_\rho \\ &\quad = B_\eta + \gamma_0[(K_\eta + \epsilon_\eta) + L_1 + L_2(K_\rho + \epsilon_\rho)] \end{aligned} \tag{95}$$

where relationships (27b), (64b), and (71c) have been used. Consider the following candidate Lyapunov function:

$$V(t) = \frac{(\rho(t) - \rho_d)^2}{2} + \frac{[\eta(t) - \eta_d(\omega_e(t), \rho(t))]^2}{2} \tag{96}$$

It follows from Eqs. (94) and (95) that for $\tilde{\mathcal{X}}_0 \in \Omega$ and $\rho(t) \ge \bar{\gamma}_b$, there exist $\alpha_1 > 0$ and $\xi_1 > 0$ such that

$$\dot{V}(t) \le -\alpha_1 V(t) + \xi_1 \tag{97a}$$

with

$$\alpha_1 = 1$$
$$\xi_1 = \frac{(B_\rho + \gamma_\rho)^2}{2} + \frac{\{B_\eta + \gamma_0[(K_\eta + \epsilon_\eta) + L_1 + L_2(K_\rho + \epsilon_\rho)]\}^2}{2} \tag{97b}$$

Considering $\mathcal{G}_2$, it follows from Eqs. (2) and (93) that $\dot{\rho}(t)$ is bounded. The frozen estimates $\bar{V}_t(t)$ and $\bar{\psi}_t(t)$ are also bounded, leading to boundedness of $\dot{\eta}(t)$ in Eq. (93) for $\rho(t) \ge \bar{\gamma}_b$. Hence, for all $\tilde{\mathcal{X}}_0 \in \Omega$ and $\rho(t) \ge \bar{\gamma}_b$, there exist positive constants M_{s_1} and M_{s_2} such that

$$|\dot{\eta}(t) - \dot{\eta}_d(\omega_e(t), \rho(t))| \le M_{s_1}, \qquad |\dot{\rho}(t)| \le M_{s_2} \tag{98}$$

Using the same candidate Lyapunov function in Eq. (96), one can have

$$\begin{aligned} \dot{V}(t) &= (\rho(t) - \rho_d)\dot{\rho}(t) + [\eta(t) - \eta_d(\omega_e(t), \rho(t))] \\ &\quad \times [\dot{\eta}(t) - \dot{\eta}_d(\omega_e(t), \rho(t))] \\ &\le M_{s_1}|\rho(t) - \rho_d| + M_{s_2}|\eta(t) - \eta_d(\omega_e(t), \rho(t))| \\ &\le \frac{(\rho(t) - \rho_d)^2}{2} + \frac{M_{s_1}^2}{2} + \frac{[\eta(t) - \eta_d(\omega_e(t), \rho(t))]^2}{2} + \frac{M_{s_2}^2}{2} \\ &= \frac{V(t)}{2} + \frac{M_{s_1}^2 + M_{s_2}^2}{2} \end{aligned} \tag{99}$$

Therefore,

$$\dot{V}(t) \le \alpha_2 V(t) + \xi_2 \tag{100a}$$

with

$$\alpha_2 = \frac{1}{2}, \qquad \xi_2 = \frac{M_{s_1}^2 + M_{s_2}^2}{2} \tag{100b}$$

D. Stability of the Closed-Loop Switched System

Combining inequalities (97a) and (100a) leads to

$$\dot{V}(t) \le \begin{cases} -\alpha_1 V(t) + \xi_1 = -\left(\alpha_1 - \frac{\xi_1}{V(t)}\right)V(t), & \text{subsystem } \mathcal{G}_1, \\ \alpha_2 V(t) + \xi_2 = \left(\alpha_2 + \frac{\xi_2}{V(t)}\right)V(t), & \text{subsystem } \mathcal{G}_2 \end{cases} \tag{101}$$

Let

$$V_b = \frac{\xi_1}{\alpha_1} + \epsilon_b$$

where $\epsilon_b > 0$ is a small positive constant. If $V(t) > V_b$,

$$\dot{V}(t) \le \begin{cases} -\lambda_0 V(t), \lambda_0 = \alpha_1 - \xi_1/V_b, & \text{subsystem } \mathcal{G}_1 \\ \mu V(t), \mu = \alpha_2 + \xi_2/V_b, & \text{subsystem } \mathcal{G}_2 \end{cases} \tag{102}$$

The next theorem establishes the stability of the closed-loop switched system consisting of the two subsystems $\mathcal{G}_1$ and $\mathcal{G}_2$.

Theorem 3: Assume that the switched system consisting of Eqs. (92) and (93) has brief instability with instability bound T_0 and asymptotic instability ratio α that satisfy

$$\alpha < \alpha^* = \frac{\lambda_0}{\lambda_0 + \mu} \tag{103a}$$

$$T_0 < \log\left(\frac{V_\Omega}{V_b}\right) \Big/ (\lambda_0 + \mu) \tag{103b}$$

where

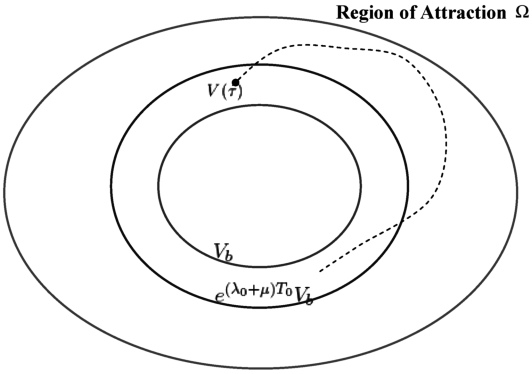

Fig. 3 Proving Lyapunov stability.

$$V_b = \frac{\xi_1}{\alpha_1} + \epsilon_b \tag{104}$$

subject to

$$0 < \epsilon_b < V_\Omega - \xi_1/\alpha_1 \tag{105}$$

with $V_\Omega = [(B_{\tilde{\rho}_0} - \gamma_\rho)^2 + (B_{\tilde{\eta}_0} - \gamma_\eta)^2]/2$ defined via $B_{\tilde{\rho}_0}$ and $B_{\tilde{\eta}_0}$ given in Eq. (58) and γ_ρ and γ_η given in Eq. (72). Then the switched system consisting of subsystems $\mathcal{G}_1$ and $\mathcal{G}_2$ is uniformly ultimately bounded with the ultimate bound given by $e^{(\lambda_0+\mu)T_0}V_b$ for all initial conditions verifying $\tilde{\mathcal{X}}_0 \in \Omega$, where Ω is given in Eq. (85).

Proof: First, note that condition (86) ensures that $\xi_1/\alpha_1 < V_\Omega$ so that the choice of ϵ_b in Eq. (105) is valid. It follows from Eqs. (104) and (105) that $V_b < V_\Omega$ and, as a result, the right-hand side of Eq. (103b) is greater than 0 so that Eq. (103b) is valid. Second, it is shown by contradiction that the trajectory of the switched system remains inside the region of attraction Ω if it starts inside Ω. Then the corresponding ultimate bound is quantified.

Since $V(0) \in \Omega$ and $V(t)$ is piecewise-continuous along the trajectory of the switched system consisting of $\mathcal{G}_1$ and $\mathcal{G}_2$, if $V(t)$ does not remain inside Ω for all $t \geq 0$, there exists $\tau_u > 0$ such that

$$V(t) \leq V_\Omega, \qquad t \in [0, \tau_u] \tag{106a}$$

$$V(\tau_u) = V_\Omega \tag{106b}$$

Since $(\rho(t) - \rho_d)^2 \leq 2V(t)$, it follows from Eq. (106a) that $|\rho(t) - \rho_d| \leq \sqrt{2V_\Omega}$ for $t \in [0, \tau_u]$, which leads to

$$\rho_d - \sqrt{2V_\Omega} \leq \rho(t)$$

Hence, the choice of

$$\rho_d \geq \sqrt{2V_\Omega} + \bar{\gamma}_b \tag{107}$$

ensures that

$$\rho(t) \geq \bar{\gamma}_b \tag{108}$$

where $\bar{\gamma}_b$ is a positive constant. It then follows from inequalities (106a) and (108) that Eqs. (97) and (100) hold. Therefore, for the V_b in Eq. (104) subject to Eq. (105), one can have

$$\begin{aligned} V(t) &\leq e^{-\lambda_0(t-\tau-T_p)+\mu T_p}V(\tau) \\ &\leq e^{-\lambda_0(t-\tau)+(\lambda_0+\mu)[T_0+\alpha(t-\tau)]}V(\tau) = e^{(\lambda_0+\mu)T_0-[\lambda_0-\alpha(\lambda_0+\mu)](t-\tau)}V(\tau) \\ &= e^{(\lambda_0+\mu)T_0-\lambda(t-\tau)}V(\tau) \end{aligned} \tag{109}$$

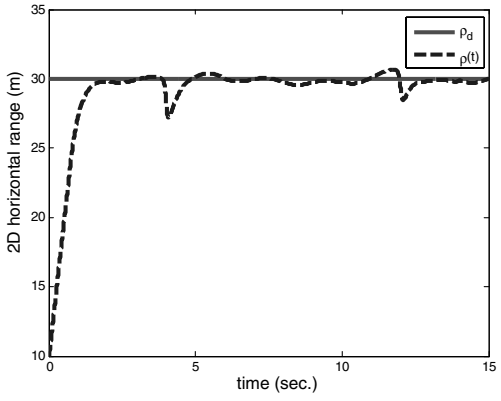

a) Relative 2D distance

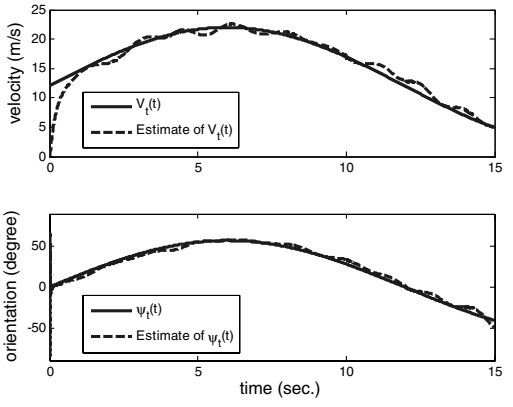

b) Estimation of target velocity

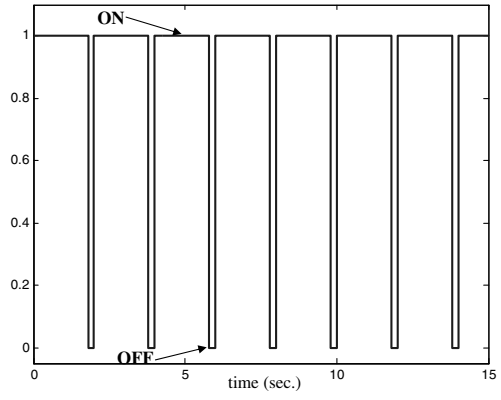

c) Switching signal (10% of a 2-second period)

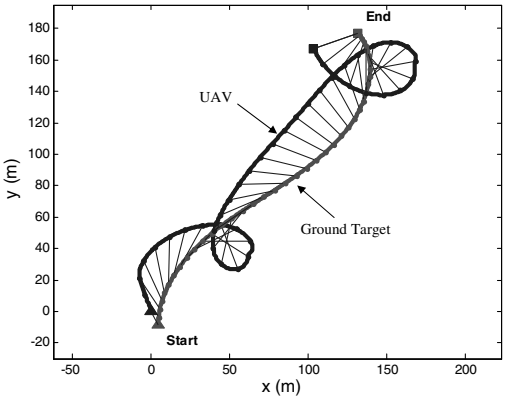

d) 2D trajectory

Fig. 4 Tracking performance of Eq. (117a) in the presence of an out-of-frame event: 10% of every 2 s.

where

$$\lambda = \lambda_0 - \alpha(\lambda_0 + \mu) \tag{110}$$

It is clear that assumption (103a) ensures that $\lambda > 0$. Next, it is shown that $V(t)$ is upper-bounded by $e^{(\lambda_0+\mu)T_0}V_b$ over $[0, \tau_u]$.

From Eq. (109), for any $V(\tau) \geq V_b$, $V(t) \leq e^{(\lambda_0+\mu)T_0-\lambda(t-\tau)}V(\tau)$, for $\tau \leq t \leq \tau_u$. Suppose that at time instant $t_1 \in [\tau, \tau_u]$,

$$V(t_1) \leq e^{(\lambda_0+\mu)T_0-\lambda(t_1-\tau)}V(\tau) \leq e^{(\lambda_0+\mu)T_0}V_b$$

Then, for any $\tau \leq t_1 \leq t_2 \leq \tau_u$,

$$\begin{aligned} V(t_2) &\leq e^{(\lambda_0+\mu)T_0-\lambda(t_2-\tau)}V(\tau) = e^{(\lambda_0+\mu)T_0-\lambda(t_1-\tau)}V(\tau)e^{-\lambda(t_2-t_1)} \\ &\leq e^{(\lambda_0+\mu)T_0}V_b e^{-\lambda(t_2-t_1)} \leq e^{(\lambda_0+\mu)T_0}V_b \end{aligned} \tag{111}$$

Hence, if $V(\tau) \geq V_b$ for any $\tau \in [0, \tau_u]$, then $V(t)$ is ultimately upper-bounded by $e^{(\lambda_0+\mu)T_0}V_b$ for $t \in [\tau, \tau_u]$. In summary, $V(t) \leq e^{(\lambda_0+\mu)T_0}V_b$, for $t \in [0, \tau_u]$. Since relationships (103b) and (105) ensure that $e^{(\lambda_0+\mu)T_0}V_b < V_\Omega$, then

$$V(t) \leq e^{(\lambda_0+\mu)T_0}V_b < V_\Omega, \quad \forall\ t \in [0, \tau_u] \tag{112}$$

which contradicts Eq. (106b). Therefore, the trajectory of the switched system remains inside Ω for all $V(0) \in \Omega$. This is illustrated in Fig. 3.

Therefore, $V(t) \in \Omega$ $(\forall\ t \geq 0)$ for any $V(0) \in \Omega$. Hence, inequalities (107–112) hold for all $t \geq 0$ and the switched system is uniformly ultimately bounded by $e^{(\lambda_0+\mu)T_0}V_b$ over Ω. This completes the proof. □

Remark 4: Recall that the adaptive system in Eq. (61) has only local stability for all $\tilde{\mathcal{X}}_0 \in \Omega$. The two inequalities (103), by restricting T_0 and α with respect to Ω, ensure that the system trajectory does not leave Ω when out-of-frame events happen. Otherwise, it is not guaranteed that the controller for $\mathcal{G}_1$ will bring the system trajectory back to Ω even when the visual measurements become available.

Remark 5: From Eqs. (103a) and (110), it can be seen that smaller α leads to larger λ and, as a result, smaller $e^{(\lambda_0+\mu)T_0-\lambda(t-\tau)}V(\tau)$. Therefore, in the presence of out-of-frame events, the tracking performance bound is upper-bounded by an exponentially growing term, with the exponent being proportional to α, so that the system has no finite escape time.

Remark 6: For $T_0 = 0$ the tradeoff between the tracking performance (represented by V_b) and the ability to handle out-of-frame events (represented by α^*) is illustrated. Recall that α^* is the upper bound on the instability ratio defined in Eq. (103a), where λ_0 and μ are given in Eq. (102). Thus,

$$\alpha^* = \frac{\lambda_0}{\lambda_0 + \mu} = \frac{1}{1 + \frac{\mu}{\lambda_0}} = \frac{1}{1 + \underbrace{\dfrac{\alpha_2 + \xi_2/V_b}{\alpha_1 - \xi_1/V_b}}_{f(V_b)}} \tag{113}$$

Consider

$$f(V_b) = \frac{\alpha_2 + \xi_2/V_b}{\alpha_1 - \xi_1/V_b} \tag{114}$$

Since

$$f'(V_b) = -\frac{1}{V_b^2}\frac{\alpha_1\xi_2 + \alpha_2\xi_1}{(\alpha_1 - \xi_1/V_b)^2} < 0 \tag{115}$$

one can have

$$V_b \text{ increases} \Rightarrow f(V_b) \text{ decreases} \Rightarrow \alpha^* \text{ increases} \tag{116}$$

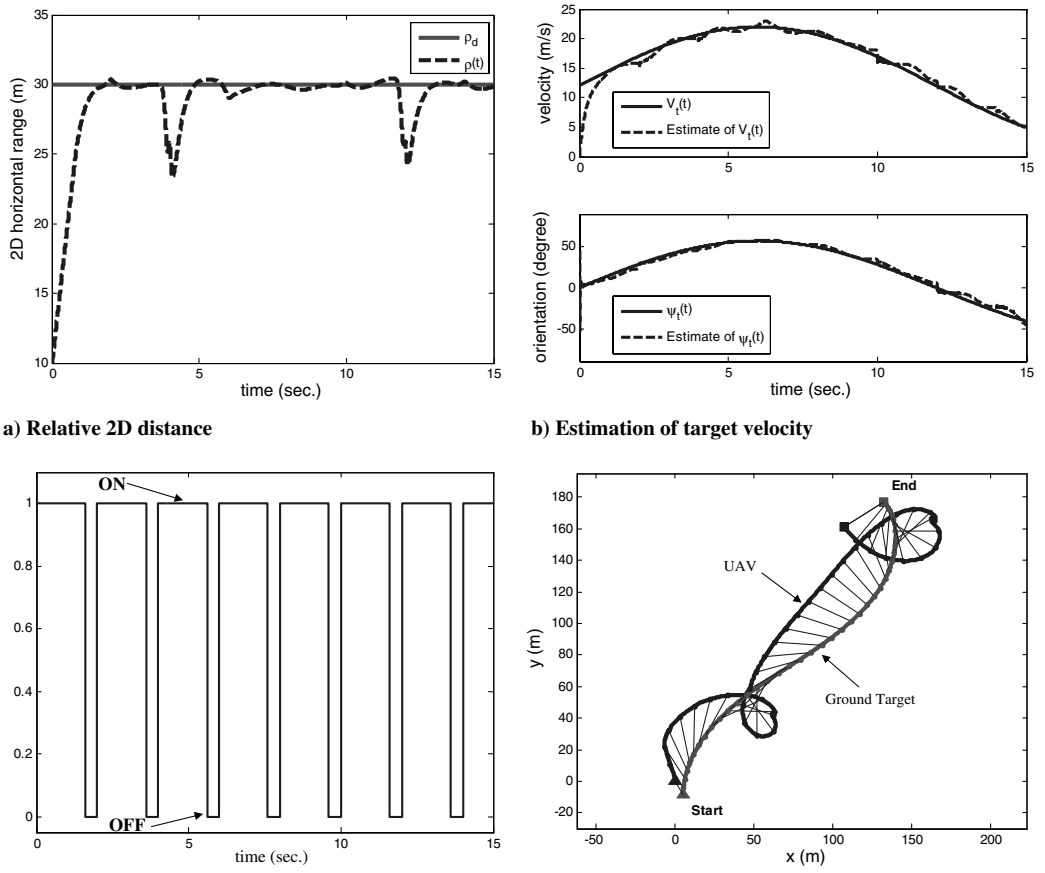

a) Relative 2D distance **b) Estimation of target velocity**

c) Switching signal (20% of a 2-second period) **d) 2D trajectory**

Fig. 5 Tracking performance of Eq. (117a) in the presence of an out-of-frame event: 20% of every 2 s.

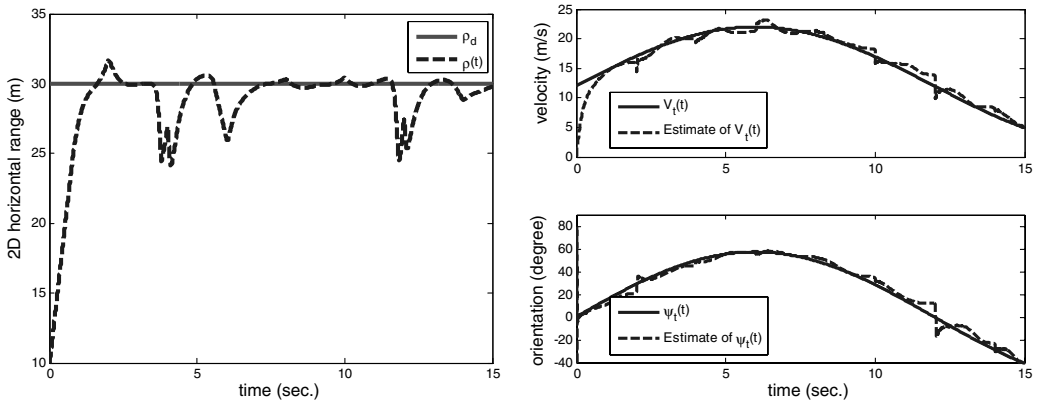

a) Relative 2D distance **b) Estimation of target velocity**

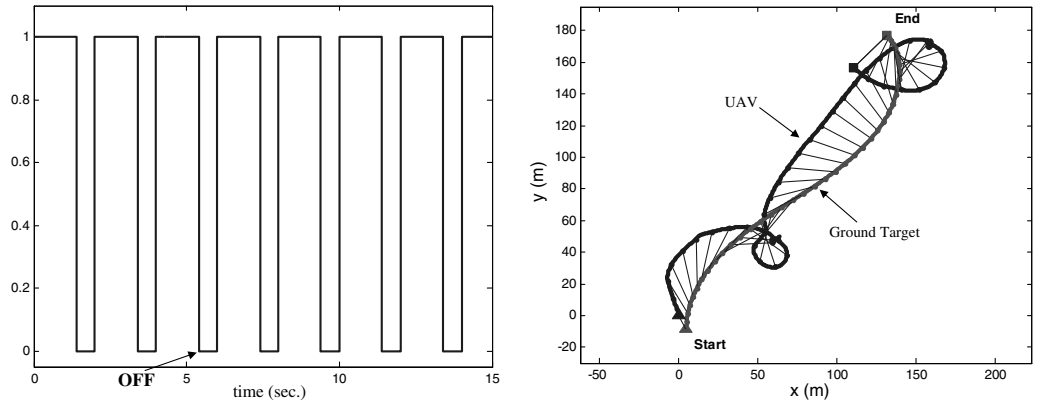

c) Switching signal (30% of a 2-second period) **d) 2D trajectory**

Fig. 6 Tracking performance of Eq. (117a) in the presence of an out-of-frame event: 30% of every 2 s.

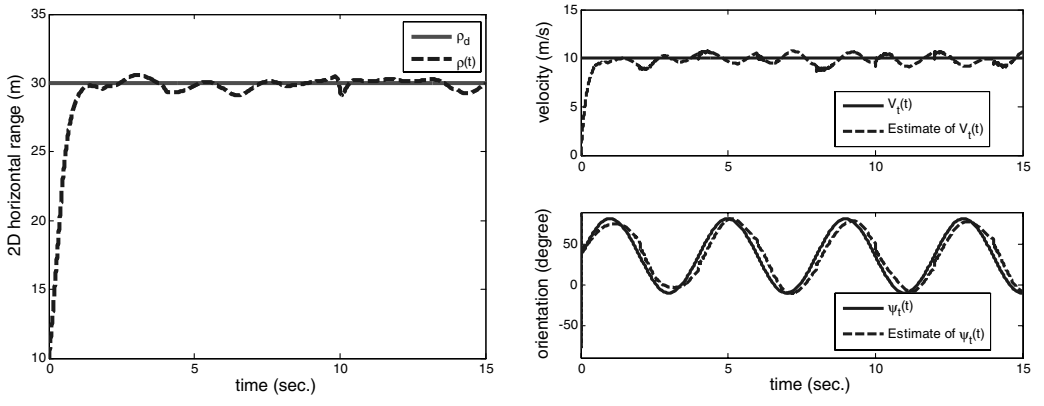

a) Relative 2D distance **b) Estimation of target velocity**

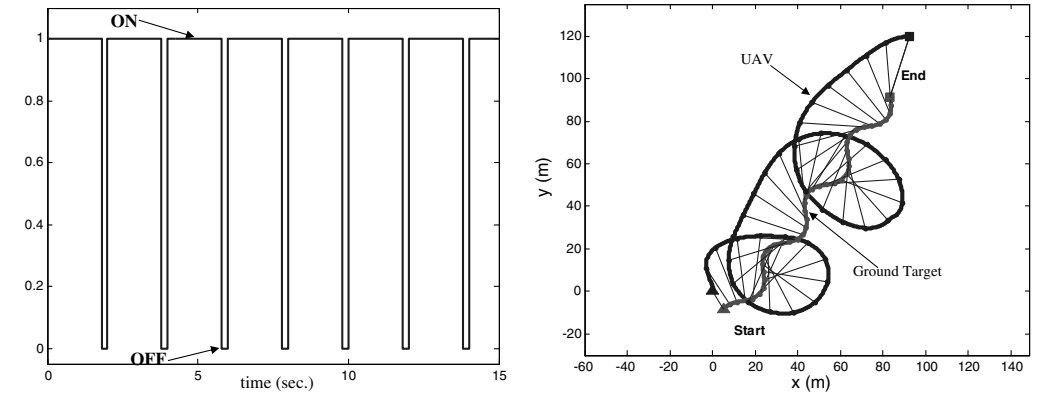

c) Switching signal (10% of a 2-second period) **d) 2D trajectory**

Fig. 7 Tracking performance of Eq. (117b) in the presence of an out-of-frame event: 10% of every 2 s.

From Eqs. (113–116), it shows that a less restrictive requirement on the tracking performance allows for a larger instability ratio.

VI. Simulations

As illustrative examples, vision-based estimation and guidance law are implemented when the target is assumed to undergo the following two different motion dynamics:

$$V_t(t) = 12 + 10\sin\left(\frac{\pi}{12}t\right), \qquad \psi_t(t) = \sin\left(\frac{\pi}{12}t\right) \tag{117a}$$

$$V_t(t) = 10, \qquad \psi_t(t) = \frac{\pi}{5} + 0.8\sin\left(\frac{\pi}{2}t\right) \tag{117b}$$

The initial conditions, estimation parameters, and control parameters are selected as follows:

1) Initial conditions are $h(t) = 100$, $\rho_d = 30$, $\rho(0) = 10$, $\eta(0) = -\pi/6$, $V_g(t) = 30$, and $\psi(0) = \pi/6$.

2) Estimation parameters are $A_m = -\mathbb{I}_{2\times 2}$, $P = \frac{1}{2}\mathbb{I}_{2\times 2}$, $\Gamma_c = 2 \times 10^6$, $c = 5$, and $\hat{\omega}(0) = (0.1, 0.1)$.

3) Control parameters are $k_1 = 3$ and $k_2 = 30$.

All quantities conform to a given unit system: for instance, meter, meters per second, etc.

In the simulations, a flat terrain is assumed. Accordingly, instead of applying Eq. (3), the target position is computed via triangulation using the measured relative altitude $h(t)$ (obtained from geolocating the target) and the measured target center $[u(t), v(t)]^\top$ (extracted by the onboard image-processing algorithm). These measurements are simulated by corrupting their true values according to

$$\begin{cases} h(t)_{\text{measure}} = (1 + 0.01\texttt{randn})h_{\text{true}}, \\ \begin{bmatrix} u(t) \\ v(t) \end{bmatrix}_{\text{measure}} = (1 + \sin(\pi t))\begin{bmatrix} u(t) \\ v(t) \end{bmatrix}_{\text{true}} \end{cases} \tag{118}$$

where `randn()` denotes the MATLAB function that generates normally distributed random numbers. Note that $h(t)_{\text{measure}}$ is not constant, since `randn()` outputs a new value at every sample time.

Figures 4–6 show the tracking performance of the switched system when the out-of-frame signal is at 10, 20, and 30% of every 2 s time interval for the target's velocity given in Eq. (117a). Figure 4a shows the regulation of the 2-D horizontal range. Figure 4b shows estimation of the ground target's velocity and orientation. Figure 4c gives the switching signal, where the out-of-frame signal $s(t)$ is at 10% of every 2 s time interval. Figure 4d plots the 2-D trajectories of the UAV and the target, where the thin lines connecting the UAV and the target indicate the corresponding positions of these two agents at some time instances, for illustration.

Figures 7–9 show another set of simulation for the target's velocity in Eq. (117b) using the same design. It can be observed from Figs. 4–9 that the tracking objective is achieved. The system performance degrades as the out-of-frame duration increases.

Using motion (117b) as an example, Fig. 10 illustrates how the tracking performance would be affected by different selections of the controller gains, without either measurement noise or out-of-frame event. In Fig. 10a, the controller gain k_1 is selected to be 1, 3, and 10, respectively, and k_2 is fixed to be $k_2 = 30$. It can be observed from Eq. (26) that k_1 should largely affect the transient speed of $\rho(t)$ approaching ρ_d, which is demonstrated by the simulation. Clearly, increasing k_1 results in faster tracking. Similarly, the effect of the controller gain k_2 on the tracking performance is given in Fig. 10b, where k_2 is chosen to be 10, 30, and 100, respectively, and k_1 stays fixed. It can be observed that increasing k_2 reduces the tracking error,

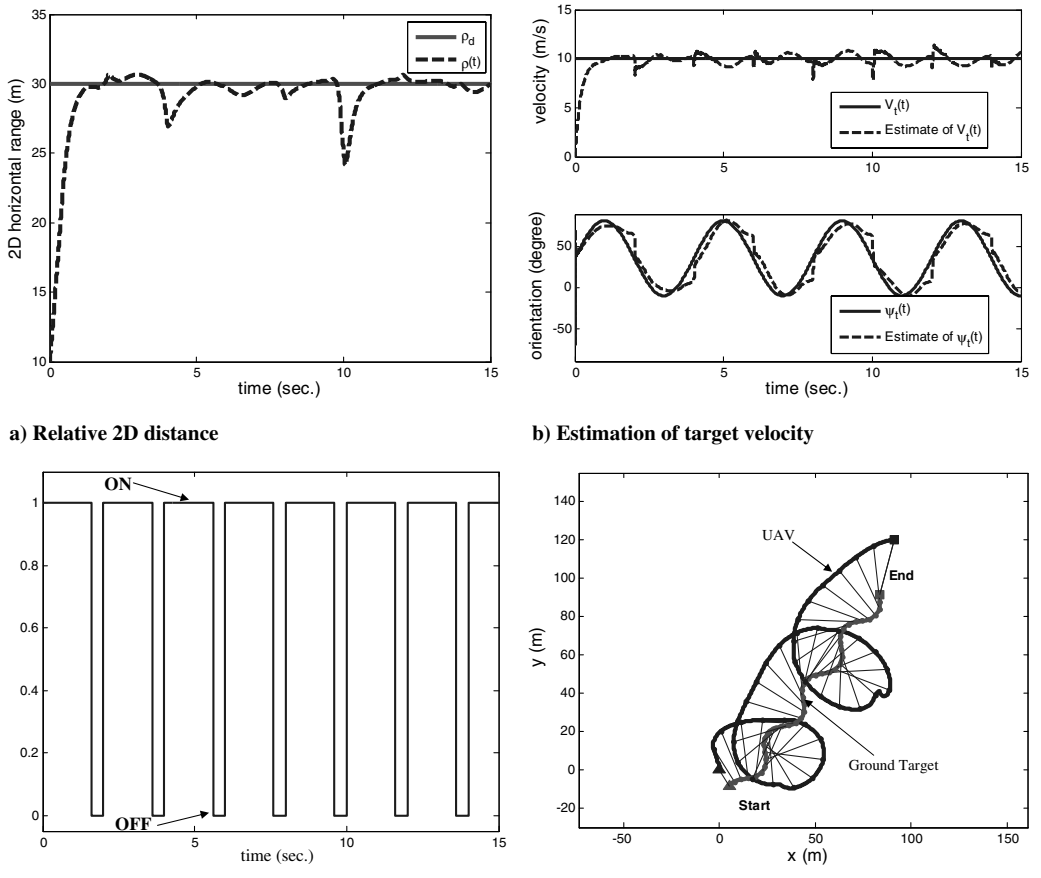

a) Relative 2D distance **b) Estimation of target velocity**

c) Switching signal (20% of a 2-second period) **d) 2D trajectory**

Fig. 8 Tracking performance of Eq. (117b) in the presence of an out-of-frame event: 20% of every 2 s.

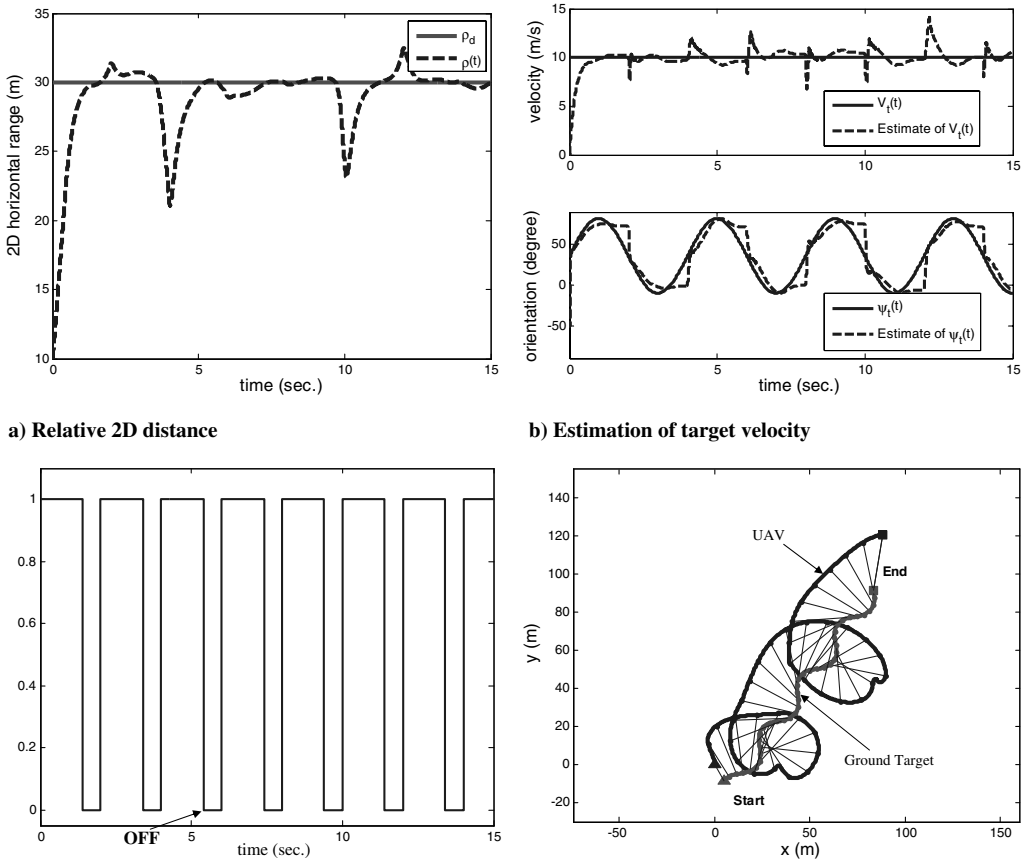

a) Relative 2D distance **b) Estimation of target velocity**

c) Switching signal (30% of a 2-second period) **d) 2D trajectory**

Fig. 9 Tracking performance of Eq. (117b) in the presence of an out-of-frame event: 30% of every 2 s.

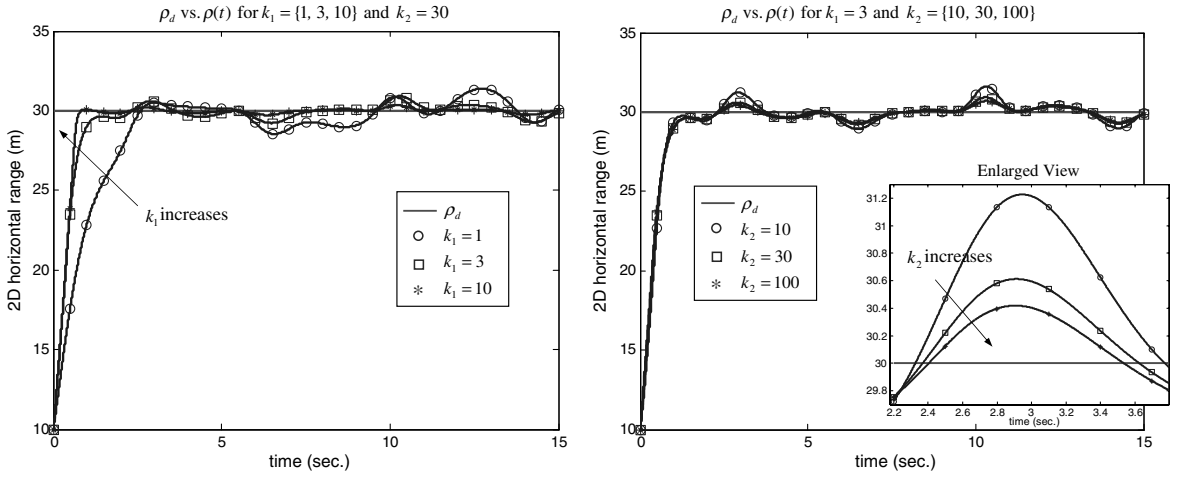

a) k_1 changes **b) k_2 changes**

Fig. 10 Tracking performance vs controller gains k_1 and k_2.

which is consistent with the tracking performance bound derived in Eq. (26), since k_2 appears in the denominator of the final tracking bound B_ρ.

Using motion (117b) as an example, Figs. 11 and 12 illustrate how the estimation performance would be affected by different selections of estimation gains, without either measurement noise or out-of-frame event. In Fig. 11, the adaptation gain Γ_c is selected to be 2×10^2, 2×10^4, and 2×10^6, respectively, and c in $C(s)$ is fixed to be $c = 5$. In Fig. 12, c is selected to be 1, 5, and 50, respectively, and Γ_c is fixed to be $\Gamma_c = 2 \times 10^6$. It can be observed from Figs. 11 and 12 that increasing either Γ_c or c improves the estimation performance.

VII. Conclusions

This paper discusses vision-based target tracking of a ground vehicle moving with unknown time-varying velocity. The control objective is to regulate the two-dimensional horizontal range between the unmanned aerial vehicle and the target to a constant. An adaptive guidance law is developed that involves a fast-estimation

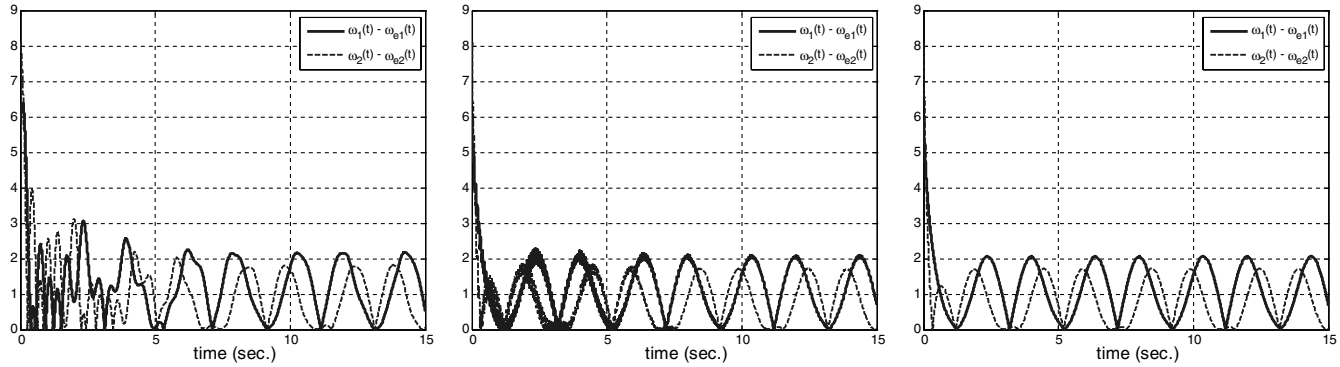

a) $\Gamma_c = 2 \times 10^2$ **b)** $\Gamma_c = 2 \times 10^4$ **c)** $\Gamma_c = 2 \times 10^6$

Fig. 11 Estimation performance vs adaptation gain Γ_c.

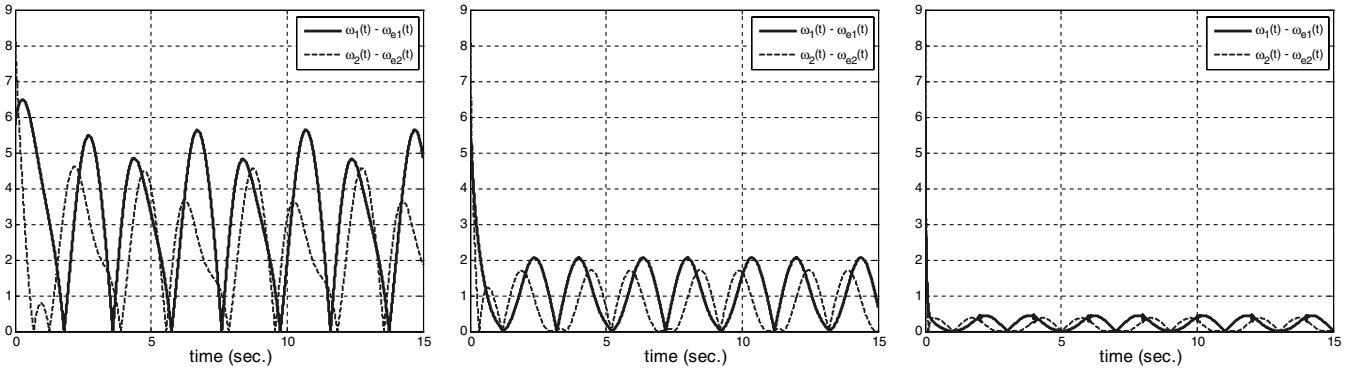

a) $c = 1$ **b)** $c = 5$ **c)** $c = 50$

Fig. 12 Estimation performance vs low-pass filter parameter c in $C(s)$.

scheme and an inverse-kinematic-based guidance law. The tracking performance bound is explicitly derived as a function of the estimation error. The paper also analyzes the stability and the performance degradation of the closed-loop adaptive system in the presence of out-of-frame events, modeled as brief instabilities. A sufficient condition for the switching signal is derived that guarantees graceful degradation of tracking performance during target loss. In summary, the paper has complete performance and robustness analysis of the vision-based target tracking in the presence of out-of-frame events.

Appendix A: Basic Definitions

Some basic definitions from linear systems theory are reviewed below.

Definition 1: For a signal $\xi(t)$ ($t \geq 0$ and $\xi(t) \in \mathbb{R}^n$), its truncated $\mathcal{L}_\infty$-norm and $\mathcal{L}_\infty$-norms are defined as

$$\|\xi_t\|_{\mathcal{L}_\infty} = \max_{i=1,\ldots,n} \left(\sup_{0 \leq \tau \leq t} |\xi_i(\tau)| \right) \tag{A1a}$$

$$\|\xi\|_{\mathcal{L}_\infty} = \max_{i=1,\ldots,n} \left(\sup_{\tau \geq 0} |\xi_i(\tau)| \right) \tag{A1b}$$

where $\xi_i(t)$ is the ith component of $\xi(t)$.

Definition 2: The $\mathcal{L}_1$-norm of a stable proper single-input/single-output system $H(s)$ is defined as

$$\|H(s)\|_{\mathcal{L}_1} = \int_0^\infty |h(t)|\, \mathrm{d}t \tag{A2}$$

where $h(t)$ is the impulse response of $H(s)$.

Definition 3: For an asymptotically stable and proper m-input/n-output system $H(s)$, the $\mathcal{L}_1$-norm is defined as

$$\|H(s)\|_{\mathcal{L}_1} = \max_{i=1,\ldots,n} \left(\sum_{j=1}^{m} \|H_{ij}(s)\|_{\mathcal{L}_1} \right)$$

where $H_{ij}(s)$ is the ith row and jth column entry of $H(s)$.

Appendix B: Lemma 1

Lemma 1: Consider a linear time-varying system:

$$\dot{x}(t) = -a(t)x(t) + \varrho(t) + b(t), \qquad x(0) = 0 \tag{B1}$$

where

$$|\varrho(t)| \leq a_0 |x(t)|, \qquad 0 < a_l \leq a(t) - a_0 \leq a_u, \qquad |b(t)| \leq b \tag{B2}$$

and a_l, a_u, a_0, and b are positive constants. Then,

$$|x(t)| \leq \frac{b}{a_l} \quad \forall\ t \geq 0 \tag{B3}$$

Proof: Since $x(0) = 0$ and $x(t)$ is continuous, if Eq. (B3) is not true, there exists $\tau \geq 0$ such that

$$x(\tau) = \frac{b}{a_l} \tag{B4a}$$

$$\dot{x}(\tau) > 0 \tag{B4b}$$

or

$$x(\tau) = -\frac{b}{a_l} \tag{B5a}$$

$$\dot{x}(\tau) < 0 \tag{B5b}$$

It follows from Eqs. (B2) and (B4a) that

$$\dot{x}(\tau) = -a(\tau)x(\tau) + \varrho(\tau) + b(\tau) \le \frac{b}{a_l}(-a(\tau) + a_0) + b$$
$$\le \frac{b}{a_l}(-a_l) + b \le 0 \tag{B6}$$

which implies $\dot{x}(\tau) \le 0$ and further contradicts Eq. (B4b). Similarly, it follows from Eqs. (B2) and (B4a) that

$$\dot{x}(\tau) = -a(\tau)x(\tau) + \varrho(\tau) + b(\tau) \ge \frac{b}{a_l}(a(\tau) - a_0) - b$$
$$\ge a_l\frac{b}{a_l} - b \ge 0 \tag{B7}$$

which implies $\dot{x}(\tau) \ge 0$ and further contradicts Eq. (B5b). Therefore, inequality (B3) must be true. □

Appendix C: About Initial Conditions

First, the choice of k_2 in Eq. (23a) leads to

$$(M_{\rho_r} + M_d(k_1))M_{\beta_1 r}/(k_1k_2) < L_{\beta_1 r}(1-\epsilon)/(8k_1)$$

Second, it follows from Eqs. (12), (22c), and (23b) that

$$\frac{(M_{\beta_1}\mu_{\beta_2} + \mu_{\beta_1})\gamma_{c\omega}}{k_1} = \frac{(M_{\beta_1}\mu_{\beta_2} + \mu_{\beta_1})}{k_1}\|1 - C(s)\|_{\mathcal{L}_1}\|\omega\|_{\mathcal{L}_\infty}$$
$$< \frac{(M_{\beta_1}\mu_{\beta_2} + \mu_{\beta_1})}{k_1}\frac{L_{\beta_1 r}(1-\epsilon)}{8M_t(M_{\beta_1}\mu_{\beta_2} + \mu_{\beta_1})}\left\|V_t(t)\begin{bmatrix}\sin\psi_t(t)\\ \cos\psi_t(t)\end{bmatrix}\right\|_{\mathcal{L}_\infty}$$
$$< \frac{L_{\beta_1 r}(1-\epsilon)}{8k_1}\frac{|V_t(t)|_\infty}{M_t} < \frac{L_{\beta_1 r}(1-\epsilon)}{8k_1}$$

Third, inequality (24a) ensures that

$$(M_{\beta_1}\mu_{\beta_2} + \mu_{\beta_1})\|\hat{\omega}_0 - \omega_0\|_\infty/k_1 < L_{\beta_1 r}(1-\epsilon)/(4k_1)$$

Thus, $B_0 < L_{\beta_1 r}(1-\epsilon)/(2k_1)$ and the right-hand side of inequality (24b) is greater than $L_{\beta_1 r}(1-\epsilon)/(2k_1)$.

Appendix D: Derivation of $\gamma_{r_1}(t)$

It is shown in this section that inequality (28) holds under conditions (23a) and (24c). Let

$$g(t) = |\tilde{\rho}_0|e^{-k_1 t} + \frac{M_{\beta_1 r}|\tilde{\eta}_0|}{k_1 - k_2}(e^{-k_2 t} - e^{-k_1 t})$$
$$\tilde{\rho}_0 = \rho_r(0) - \rho_d$$
$$\tilde{\eta}_0 = \eta_r(0) - \eta_d(\omega_r(0), \rho_r(0)) \tag{D1}$$

Compute $\dot{g}(t)$ from Eq. (D1):

$$\dot{g}(t) = \frac{k_2 M_{\beta_1 r}|\tilde{\eta}_0|}{k_2 - k_1}e^{-k_2 t} - \left(\frac{k_1 M_{\beta_1 r}|\tilde{\eta}_0|}{k_2 - k_1} + k_1|\tilde{\rho}_0|\right)e^{-k_1 t}$$
$$= \frac{k_2 M_{\beta_1 r}|\tilde{\eta}_0|}{k_2 - k_1}(e^{-k_2 t} - e^{-k_1 t}) + (M_{\beta_1 r}|\tilde{\eta}_0| - k_1|\tilde{\rho}_0|)e^{-k_1 t} \tag{D2}$$

It follows from Eqs. (23a), (24c), and (D2) that $\dot{g}(t) < 0$ for all $t \ge 0$. Thus, $g(t)$ achieves its maximum value at $t = 0$. Moreover, the signal

$$\frac{M_{\beta_1}\mu_{\beta_2} + \mu_{\beta_1}}{k_1}\|\omega_0 - \hat{\omega}_0\|_\infty e^{-ct}$$

decreases monotonically for all $t \ge 0$. Therefore, it follows from Eq. (27a) that

$$\gamma_{r_1}(t) = g(t) + \frac{M_{\beta_1}\mu_{\beta_2} + \mu_{\beta_1}}{k_1}\|\omega_0 - \hat{\omega}_0\|_\infty e^{-ct} + B_\rho$$
$$\le g(0) + \frac{M_{\beta_1}\mu_{\beta_2} + \mu_{\beta_1}}{k_1}\|\omega_0 - \hat{\omega}_0\|_\infty + B_\rho$$
$$= |\rho_r(0) - \rho_d| + B_0 = \bar{\gamma}_{r_1} \tag{D3}$$

Thus, relationship (28) holds under Eqs. (23a) and (24c).

Appendix E: Choice of ρ_d

The choice of ρ_d in Eq. (25) says that ρ_d needs to be selected to satisfy

$$\rho_d \ge \bar{\gamma}_{r_1} + \gamma_b = |\rho_r(0) - \rho_d| + B_0 + \gamma_b \tag{E1}$$

1) If $\rho_r(0) \ge \rho_d$, choosing $\rho_d \ge [\rho_r(0) + B_0 + \gamma_b]/2$ leads to Eq. (E1) directly.

2) If $\rho_r(0) < \rho_d$, it follows from Eq. (24d) that

$$B_0 + \gamma_b < \rho_r(0) \Rightarrow \rho_d - \rho_r(0) + B_0 + \gamma_b < \rho_d$$
$$\Rightarrow |\rho_d - \rho_r(0)| + B_0 + \gamma_b < \rho_d \tag{E2}$$

Thus, Eq. (E1) holds.

Appendix F: Derivation of $\Delta_\rho(t)$ and $\Delta_\eta(t)$

Suppose there exist finite constants $L_1, L_2, \mu_\rho, M_{\rho_1}$, and M_{ρ_2} such that Eqs. (64b) and (64c) hold. Consider Eq. (63a) and rewrite it as

$$\dot{\tilde{\rho}}(t) = -k_1\tilde{\rho}(t) + \underbrace{\Delta_{\rho_1}(t) + \Delta_{\rho_2}(t)}_{\Delta_\rho(t)} \tag{F1}$$

where

$$\Delta_{\rho_1}(t) = \beta_1(\omega(t))[\sin(\eta(t) + \beta_2(\omega(t))) - \sin(\eta_r(t) + \beta_2(\omega(t)))]$$
$$\Delta_{\rho_2}(t) = \beta_1(\omega_r(t))\sin(\eta_d(\omega_r(t), \rho_r(t)) + \beta_2(\omega_r(t)))$$
$$- \beta_1(\omega_e(t))\sin(\eta_d(\omega_e(t), \rho(t)) + \beta_2(\omega_e(t))) \tag{F2}$$

One can have

$$|\Delta_{\rho_1}(t)| = M_{\beta_1}|\eta(t) - \eta_r(t)|$$
$$|\Delta_{\rho_2}(t)| = |\beta_1(\omega_r(t))\sin(\eta_d(\omega_r(t), \rho_r(t)) + \beta_2(\omega_r(t)))$$
$$- \beta_1(\omega_r(t))\sin(\eta_d(\omega_e(t), \rho(t)) + \beta_2(\omega_e(t)))$$
$$+ \beta_1(\omega_r(t))\sin(\eta_d(\omega_e(t), \rho(t)) + \beta_2(\omega_e(t)))$$
$$- \beta_1(\omega_e(t))\sin(\eta_d(\omega_e(t), \rho(t)) + \beta_2(\omega_e(t)))|$$
$$\le M_{\beta_1 r}|\eta_d(\omega_e(t), \rho(t)) - \eta_d(\omega_r(t), \rho_r(t))|$$
$$+ (M_{\beta_1 r}\mu_{\beta_2} + \mu_{\beta_1})\|\omega_e(t) - \omega_r(t)\|_\infty$$
$$\le M_{\beta_1 r}L_2|\rho(t) - \rho_r(t)| + (M_{\beta_1 r}L_1 + M_{\beta_1 r}\mu_{\beta_2} + \mu_{\beta_1})$$
$$\times \|\omega_e(t) - \omega_r(t)\|_\infty \tag{F3}$$

where M_{β_1}, $M_{\beta_1 r}$, μ_{β_1}, μ_{β_2}, L_1, and L_2 are given in Eqs. (22c) and (64), respectively. From the above, inequality (66a) holds by choosing κ_i (for $i = 1, 2, 3$) as

$$\kappa_1 = M_{\beta_1 r}L_2, \qquad \kappa_2 = M_{\beta_1}, \qquad \kappa_3 = M_{\beta_{1r}} + M_{\beta_1 r}\mu_{\beta_2} + \mu_{\beta_1} \tag{F4}$$

Next, consider Eq. (63b) and rewrite it to be

$$\dot{\tilde{\eta}}(t) = -k_2\tilde{\eta}(t) + \underbrace{\Delta_{\eta_1}(t) + \Delta_{\eta_2}(t) + k_2(\eta_d(\omega_e(t)) - \eta_d(\omega_r(t)))}_{\Delta_\eta(t)} \tag{F5}$$

where

$$\Delta_{\eta_1}(t) = \frac{\hat{V}_t(t)\cos(\hat{\psi}_t(t) - \psi(t) + \eta(t))}{\rho(t)} - \frac{V_r(t)\cos(\psi_r(t) - \psi(t) + \eta_r(t))}{\rho_r(t)}$$
$$\Delta_{\eta_2}(t) = \frac{V_t(t)\cos(\psi_t(t) - \psi(t) + \eta(t))}{\rho(t)} - \frac{V_t(t)\cos(\psi_t(t) - \psi(t) + \eta_r(t))}{\rho_r(t)} \tag{F6}$$

Since

$$\begin{aligned}\Delta_{\eta_1}(t) &= \frac{\hat{V}_t(t)\cos(\hat{\psi}_t(t) - \psi(t) + \eta(t))}{\rho(t)} - \frac{\hat{V}_t(t)\cos(\psi_r(t) - \psi(t) + \eta_r(t))}{\rho(t)} + \frac{\hat{V}_t(t)\cos(\psi_r(t) - \psi(t) + \eta_r(t))}{\rho(t)} - \frac{V_r(t)\cos(\psi_r(t) - \psi(t) + \eta_r(t))}{\rho_r(t)} \\ &= \frac{\hat{V}_t(t)}{\rho(t)}[\cos(\hat{\psi}_t(t) - \psi(t) + \eta(t)) - \cos(\psi_r(t) - \psi(t) + \eta_r(t))] \\ &\quad + \cos(\psi_r(t) - \psi(t) + \eta_r(t))\left(\frac{\hat{V}_t(t)}{\rho(t)} - \frac{V_r(t)}{\rho_r(t)}\right) \\ &= -2\frac{\hat{V}_t(t)}{\rho(t)}\sin\left(\frac{\hat{\psi}_t(t) + \eta(t) + \psi_r(t) + \eta_r(t)}{2} - \psi(t)\right) \\ &\quad \times \sin[(\hat{\psi}_t(t) - \psi_r(t)) + (\eta(t) - \eta_r(t))] \\ &\quad + \frac{\hat{V}_t(t)}{\rho(t)\rho_r(t)}(\rho_r(t) - \rho(t)) + \frac{1}{\rho_r(t)}(\hat{V}_t(t) - V_r(t))\end{aligned} \tag{F7}$$

and

$$\begin{aligned}\Delta_{\eta_2}(t) &= V_t(t)\left[\frac{1}{\rho(t)}\cos(\psi_t(t) - \psi(t) + \eta(t)) - \frac{1}{\rho(t)}\cos(\psi_t(t) - \psi(t) + \eta_r(t))\right] + V_t(t)\left[\frac{1}{\rho(t)}\cos(\psi_t(t) - \psi(t) + \eta_r(t)) - \frac{1}{\rho_r(t)}\cos(\psi_t(t) - \psi(t) + \eta_r(t))\right] \\ &= \frac{-2V_t(t)}{\rho(t)}\sin\left(\psi_t(t) - \psi(t) + \frac{\eta(t) + \eta_r(t)}{2}\right)\sin(\eta(t) - \eta_r(t)) + \frac{V_t(t)\cos(\psi_t(t) - \psi(t) + \eta_r(t))}{\rho(t)\rho_r(t)}(\rho_r(t) - \rho(t))\end{aligned} \tag{F8}$$

it follows from Eq. (22c) that

$$\begin{aligned}|\Delta_\eta(t)| &= |\Delta_{\eta_1}(t) + \Delta_{\eta_2}(t) + \Delta_{\eta_3}(t)| \\ &\le 2\frac{\hat{V}_t(t)}{\rho(t)}[|\hat{\psi}_t(t) - \psi_r(t)| + |\eta(t) - \eta_r(t)|] + \frac{\hat{V}_t(t)}{\rho(t)\rho_r(t)}|\rho(t) - \rho_r(t)| + \frac{1}{\rho(t)}|\hat{V}_t(t) - V_r(t)| \\ &\quad + 2\frac{V_t(t)}{\rho(t)}|\eta(t) - \eta_r(t)| + \frac{V_t(t)}{\rho(t)\rho_r(t)}|\rho_r(t) - \rho(t)| \\ &\quad + k_2L_1\|\omega_e(t) - \omega_r(t)\|_\infty + k_2L_2|\rho(t) - \rho_r(t)| \\ &\le \frac{2(\hat{V}_t(t) + V_t(t))}{\rho(t)}|\eta(t) - \eta_r(t)| + \left(\frac{\hat{V}_t(t) + V_t(t)}{\rho(t)\rho_r(t)} + k_2L_2\right)|\rho(t) - \rho_r(t)| + \frac{1}{\rho(t)}[2\hat{V}_t(t)|\hat{\psi}_t(t) - \psi_r(t)| + |\hat{V}_t(t) - V_r(t)|] + k_2L_1\|\omega_e(t) - \omega_r(t)\|_\infty\end{aligned} \tag{F9}$$

It follows from Eqs. (64) and (F9) that there exist finite constants κ_i (for $i = 3, 4, 5$), chosen as

$$\kappa_4 = M_{\rho_1}, \qquad \kappa_5 = M_{\rho_2} + k_2L_2, \qquad \kappa_6 = \mu_\rho + k_2L_1 \tag{F10}$$

such that inequality (66b) holds.

Appendix G: About $B_{\tilde{\omega}_0} - \gamma_0$

The choice of Γ_c in Eq. (69b) leads to $B_{\tilde{\omega}_0} - \gamma_0 > 0$ directly. Thus, the right-hand side of Eq. (70a) is greater than 0. It follows from Eqs. (60a) and (69b) that

$$\sqrt{\Gamma_c} > \frac{2(K_\rho + \epsilon_\rho)\gamma_c}{B_{\tilde{\rho}_0} - B_\rho} > \frac{(K_\rho + \epsilon_\rho)\gamma_c}{B_{\tilde{\rho}_0}}$$
$$\Rightarrow B_{\tilde{\rho}_0} - (K_\rho + \epsilon_\rho)\frac{\gamma_c}{\sqrt{\Gamma_c}} > 0 \Rightarrow B_{\tilde{\rho}_0} - \gamma_\rho > 0$$

Thus, the right-hand side of Eq. (70b) is greater than 0. Similarly, it can be shown that the right-hand side of Eq. (70c) is greater than 0.

Acknowledgments

The work was sponsored in part by the U.S. Army Research Office grant W911NF-06-1-0330 and U.S. Air Force Office of Scientific Research Multidisciplinary University Research Initiative subcontract F49620-03-1-0401. Authors from the Naval Postgraduate School acknowledge the support of the U.S. Special Operations Command.

References

[1] Dobrokhodov, V., Kaminer, I., Jones, K., and Ghabcheloo, R., "Vision-Based Tracking and Motion Estimation for Moving Targets Using Unmanned Air Vehicles," *Journal of Guidance, Control, and Dynamics*, Vol. 31, No. 4, July–Aug. 2008, pp. 907–917. doi:10.2514/1.33206

[2] Wang, I., Dobrokhodov, V., Kaminer, I., and Jones, K., "On Vision-Based Target Tracking and Range Estimation for Small UAVs," AIAA Guidance, Navigation and Control Conference, San Francisco, AIAA Paper 2005-6401, Aug. 2005.

[3] Dobrokhodov, V., Kaminer, I., Jones, K., and Ghabcheloo, R., "Vision-Based Tracking and Motion Estimation for Moving Targets Using Small UAVs," AIAA Guidance, Navigation and Control Conference, Keystone, CO, AIAA Paper 2006-6606, Aug. 2006.

[4] Kaminer, I., Kang, W., Yakimenko, O., and Pascoal, A., "Application of Nonlinear Filtering To Navigation System Design Using Passive Sensors," *IEEE Transactions on Aerospace and Electronic Systems*, Vol. 37, No. 1, Jan. 2001, pp. 158–172. doi:10.1109/7.913675

[5] Hespanha, J., Yakimenko, O., Kaminer, I., and Pascoal, A., "Linear Parametrically Varying Systems with Brief Instabilities: An Application to Integrated Vision/IMU Navigation," *IEEE Transactions on Aerospace and Electronic Systems*, Vol. 40, No. 3, July 2004, pp. 889–902. doi:10.1109/TAES.2004.1337462

[6] Pascoal, A., Kaminer, I., and Oliveira, P., "Navigation System Design Using Time-Varying Complementary Filters," *IEEE Transactions on Aerospace and Electronic Systems*, Vol. 36, No. 4, Oct. 2000, pp. 1099–1114. doi:10.1109/7.892661

[7] Dobrokhodov, V., Kaminer, I., Jones, K., Kitsios, I., Cao, C., Ma, L., Hovakimyan, N., and Woolsey, C., "Rapid Motion Estimation of a Target Moving with Time-Varying Velocity," AIAA Guidance, Navigation and Control Conference, Hilton Head, SC, AIAA Paper 2007-6746, Aug. 2007.

[8] Ma, L., Cao, C., Hovakimyan, N., Woolsey, C., Dobrokhodov, V., and Kaminer, I., "Development of a Vision-Based Guidance Law for Tracking a Moving Target," AIAA Guidance, Navigation and Control Conference, Hilton Head, SC, AIAA Paper 2007-6744, Aug. 2007.

[9] Liberzon, D., *Switching in Systems and Control*, Kluwer Academic, Norwell, MA, June 2003.

[10] Sridhar, B., and Suorsa, R., "Vision-Based Obstacle Detection for Rotocraft Flight," *Journal of Robotic Systems*, Vol. 9, No. 6, 1992, pp. 709–727. doi:10.1002/rob.4620090603

[11] Suorsa, R., and Sridhar, B., "A Parallel Implementation of a Multisensor Feature-Based Range-Estimation Method," *IEEE Transactions on Robotics and Automation*, Vol. 10, No. 6, 1994, pp. 755–768. doi:10.1109/70.338530

[12] Petillot, Y., Ruiz, I., and Lane, D., "Underwater Vehicle Obstacle Avoidance and Path Planning Using a Multi-Beam Forward Looking Sonar,"*IEEE Journal of Oceanic Engineering*, Vol. 26, No. 2, pp. 240–251. doi:10.1109/48.922790, 2001.

[13] Costa, P., "Adaptive Model Architecture and Extended Kalman-Bucy Filters," *IEEE Transactions on Aerospace and Electronic Systems*, Vol. 30, No. 2, 1994, pp. 525–533. doi:10.1109/7.272275

[14] Farina, D., and Ristic, B., "Tracking a Ballistic Target: Comparison of Several Nonlinear Filters," *IEEE Transactions on Aerospace and Electronic Systems*, Vol. 38, No. 3, pp. 854–867. doi:10.1109/TAES.2002.1039404, 2002.

[15] Christophersen, H., Pickell, R., Neidhoefer, J., Koller, A., Kannan, S., and Johnson, E., "A Compact Guidance, Navigation, and Control System for Unmanned Aerial Vehicles," *Journal of Aerospace Computing, Information, and Communication*, Vol. 3, No. 5, 2006, pp. 187–213. doi:10.2514/1.18998

[16] Langelaan, J., and Rock, S., "Navigation of Small UAVs Operating in Forests," AIAA Guidance, Navigation and Control Conference, Providence, RI, AIAA Paper 2004-5140, 2004.

[17] Langelaan, J., "State Estimation for Autonomous Flight in Cluttered Environments," *Journal of Guidance, Control, and Dynamics*, Vol. 30, No. 5, 2007, pp. 1414–1426. doi:10.2514/1.27770

[18] Zarchan, P., and Alpert, J., "Using Filter Banks to Improve Interceptor Performance Against Weaving Targets," AIAA Guidance, Navigation and Control Conference, Keystone, CO, AIAA Paper 2006-6700, 2006.

[19] Oh, S., and Johnson, E., "Relative Motion Estimation for Vision-Based Formation Flight Using Unscented Kalman Filter," AIAA Guidance, Navigation and Control Conference, Hilton Head, SC, AIAA Paper 2007-6866, 2007.

[20] Ma, L., Cao, C., Hovakimyan, N., Woolsey, C., and Dixon, W., "Fast Estimation for Range Identification in the Presence of Unknown Motion Parameters," *ICINCO-SPSMC*, Angers, France, May 2007, pp. 157–164.

[21] Ma, L., Cao, C., Hovakimyan, N., Woolsey, C., and Dixon, W., "Fast Estimation for Range Identification in the Presence of Unknown Motion Parameters," *IMA Journal of Applied Mathematics* (to be published).

[22] Dippold, A., "Vision-Based Obstacle Avoidance for Multiple Vehicles Performing Time-Critical Missions," Ph.D. Dissertation, Virginia Polytechnic Institute and State Univ., Blacksburg, VA, 2009.

[23] Ma, L., Cao, C., Hovakimyan, N., Dobrokhodov, V., and Kaminer, I., "Adaptive Vision-Based Guidance Law With Guaranteed Performance Bounds for Tracking a Ground Target with Time-Varying Velocity," AIAA Guidance, Navigation and Control Conference, AIAA Paper 2008-7445, Aug. 2008.

[24] Ghabcheloo, R., Aguiar, A., Pascoal, A., Silvestre, C., Kaminer, I., and Hespanha, J., "Coordinated Path-Following Control of Multiple Underactuated Autonomous Vehicles in the Presence of Communication Failures," *IEEE Conference on Decision and Control*, Inst. of Electrical and Electronics Engineers, Piscataway, NJ, Dec. 2006, pp. 4345–4350.

[25] Mohammadpour, J., and Grigoriadis, K., "Stability and Performance Analysis of Time Delayed Linear Parameter Varying Systems with Brief Instability," *IEEE Conference on Decision and Control*, Inst. of Electrical and Electronics Engineers, Piscataway, NJ, Dec. 2007, pp. 2779–2784.